SEMANTIC

end-to-end Slicing and data-drivEn autoMAtion of Next generation cellular neTworks with mobIle edge Clouds

Marie Skłodowska-Curie Actions (MSCA)
Innovative Training Networks (ITN)
H2020-MSCA-ITN-2019
861165 – SEMANTIC

WP1 – Spectrum and Forward-Compatibility Aspects for multi-GHz NR operation

D1.1: Recent trends and SotA techniques for multi-GHz radio (M18)

Contractual Date of Delivery:	M18
Actual Date of Delivery:	30/06/2021
Responsible Beneficiary:	UOA
Contributing beneficiaries:	UOA, CLM, NI, CTTC
Security:	Public
Nature:	Report
Version:	V2.1

Document Information

Version Date: 22/06/2021
Total Number of Pages: 62

Authors

Name	Organization	Email
Dr. Nikos Passas	UOA	passas@di.uoa.gr
Paraskevi Papadopoulou	UOA	vivian@uoa.gr
Azadeh Tabeshnezhad	CLM	azadeh.tabeshnezhad@chalmers.se
Mehdi Sattari	CLM	mehdi.sattari@chalmers.se
Prof. Tommy Svensson	CLM	tommy.svensson@chalmers.se
Dr. Abdo Gaber	NI	abdo.gaber@ni.com
Prof. Lazaros Merakos	UOA	merakos@di.uoa.gr
Dr. Dionysis Xenakis	FOG	dionysis@fogus.gr

Document History

Revision	Date	Modification	Contact Person
V1.0	27/03/2021	Defining a preliminary table of contents	Dr. Dionysis Xenakis
V1.1	25/05/2021	Merging contributions of all ESRs	Mrs. Paraskevi Papadopoulou
V2.0	01/06/2021	Editor changes	Dr. Nikos Passas
V2.1	02/06/2021	Editor changes	Dr. Dionysis Xenakis


SEMANTIC

TABLE OF CONTENTS

List of Acronyms and Abbreviations

Abbreviation	Explanation
3GPP	3rd generation partnership project
4G	4th generation of wireless networks
5G	5th generation of wireless networks
5GC	5G core network
6G	6th generation of wireless networks
ADC	Analogue to digital converter
AP	Access Point
AWGN	Additive white gaussian noise
BBU	Baseband unit
BS	Base station
CF	Cell-free
CNN	Convolutional neural network
CPU	Central processing unit
CSI	Channel state information
DAS	Distributed antenna system
DCC	Dynamic cooperation clusters
D-MIMO	Distributed MIMO
DMRS	Demodulation Reference Signal
DNN	Deep neural network
DL	Downlink
eMBB	Enhanced Mobile BroadBand
EPA	Equal power allocation
ESR	Early-stage researcher
FD	Full duplex
FDD	Frequency-division duplexing
FPGA	Field-programmable gate array
gNB	g Node B (logical 5G radio node)
GPS	Global positioning system
IAB	Integrated access and backhaul
ICI	Inter-cell interference
IF	Intermediate frequency
i.i.d.	Independent and identically distributed
IRS	Intelligent reflective surface
K-NN	k-nearest neighbours
KPI	Key performance indicator
LS	Least square
LTE	Long term evolution
MA	Multiple access
MIMO	Multiple-input multiple-output

mMIMO	Massive MIMO
MMSE	Minimum mean squared error
mMTC	Massive machine-type communication
MR	Maximum Ratio
MPR	Maximal path-loss ratio
mmWave	Millimeter-wave communications
NI	National Instruments
NOMA	Non-orthogonal multiple access
NR	New radio
NS	Network slice
NSA	Non-standalone
OCXO	Oven-controlled crystal oscillator
OFDM	Orthogonal frequency-division multiplexing
OMA	Orthogonal multiple access
PA	Power allocation
PC	Personal Computer
PDF	Probability density function
PHY	Physical layer
PPP	Poisson point process
QoS	Quality of Service
RAN	Radio access network
RAT	Radio access technology
RAU	Remote antenna unit
RF	Radio frequency
RFNoC	Radio frequency Network-on-Chip
RFSoC	Radio frequency System-on-Chip
RZF	Regularized zero forcing
SA	Standalone
SC	Small cell
SCS	Subcarrier spacing
SDR	Software-defined radio
SDN	Software-defined networking
SE	Spectral efficiency
SG	Stochastic geometry
SIC	Successive interference cancellation
SLNR	Signal-to-leakage-and-noise-ratio
SOS	Second Order Statistical
SotA	State-of-the-art
TDD	Time-division duplexing
UAV	Unmanned aerial vehicle

UE	User equipment
UHD	Ultra-High Definition
UL	Uplink
ULA	Uniform linear array
UPA	Uniform planar array
URLLC	Ultra-Reliable Low-Latency Communication
USRP	Universal software radio peripheral
WMMSE	Weighted minimum mean square error
WF	Water filling
WP1	Work package 1
ZF	Zero-forcing

Table of Figures

Executive summary

This report includes the SEMANTIC ESR contributions towards the objectives of WP1 (Spectrum and Forward-Compatibility Aspects for multi-GHz NR operation). More specifically, it summarizes the key findings of the ESRs towards Task 1.1 that includes state-of-the-art (SotA) assessment and acquisition of methodological tools. This task has been led by UOA and contributing partners are NI and CLM. ESRs contributing to this deliverable are UOA-1, NI-1, CLM-1, and CLM-2. The deliverable summarizes the ESR progress towards studying existing works and standardization activities on NR, focusing on mmWave communications and FD schemes, NOMA waveforms for multi-carrier access, future trends for massive/distributed MIMO and mixed performance evaluation techniques (simulation/real-life experiments). A study on NR coexistence with other systems in high bands is also provided and mechanisms for KPI measurement are specified. Outcomes of this deliverable will be circulated to WP4 to convey to the respective ESRs a list of PHY components, resources and techniques towards the automated control and parameterization of the NR.

1. Introduction

WP1 targets Spectrum and Forward-Compatibility Aspects for multi-GHz NR operation and this report provides the SotA review on this domain. With the term 5G NR we refer to the new Radio Access technology (RAT) that is standardized by the 3rd generation partnership project (3GPP) for the 5th generation of mobile communications (5G). More specifically, WP1 aims at proposing beyond 5G transmission techniques that are 5G NR compliant but also take into account future improvements towards the 6G system (i.e., forward compatible). In doing so, it is desirable to consider the abundance of spectrum that is now made available in 5G by enabling Millimeter Wave (mmWave) communications, while at the same time addressing the potential coexistence issues that will arise when operating in multi-GHz bands. 5G NR is also supporting features like beamforming and beam management that allow the transmitted signal to have increased directivity/focus towards the destination. Therefore, beamforming techniques allow higher signal quality at the receiver making communications faster and more reliable, two very desirable features for future communication systems. WP1 further considers Multiple-Input Multiple-Output (MIMO) communications that enable beamforming features but also have a beneficial effect to the data capacity and system diversity. 5G NR includes massive MIMO (mMIMO) in the standards i.e., systems where the numbers of antennas at the base station (BS) by far exceed the number of supported users by the specific BS. Some extensions of interest to MIMO communications are Distributed MIMO (D-MIMO), which is also known as Network MIMO, where the base station (BS) antennas are distributed in an area instead of being collocated and Cell-Free (CF) mMIMO where the user can be serviced by more than one BS (a cluster of distributed BSs) in a specific area.

All the above-mentioned features are grouped in two research challenges to be addressed by WP1 as discussed in the project proposal.

Challenge A1: “Spectrum and system coexistence aspects for 5G NR operation in multi-GHz bands”

Challenge A2: “5G NR forward-compatible design and future proof enhancements”.

Each challenge is tied to two key performance indicators (KPIs) that will be addressed through each involved ESR’s topic. More specifically, challenge A1 is associated with i) achieving a peak data rate of 20 Gbps using 2 GHz bandwidth and ii) absorb 2 Tbps in a smart office environment. Challenge A2 is associated with i) achieving 99.9% service availability (or more) and ii) achieving 2Gbps as a user perceived rate in an indoor environment. In the remaining part of this section a brief overview of the 5G NR and the standardization process for 5G NR is given and a discussion of spectrum coexistence in high frequency bands along with modelling aspects of such systems are presented.

In the remainder of this section, a brief overview of 5G is given. More specifically, section 1.1 discusses 5G NR, its new features, and the improvements they bring. Section 1.2 presents the standardization bodies and the standardization process for 5G NR in terms of standardization phases and the stable releases that result from them.

1.1. Overview of 5G NR

5G mobile networks are now developing to address emerging applications requiring enhanced mobile broadband (eMBB), ultra-reliable low latency communication (URLLC), and massive machine-type communication (mMTC) [1]. To enable delivering high data rate and reliable low latency connectivity, exploiting new radio spectrum and massive antenna arrays are a prerequisite for physical layer operations. Furthermore, dynamic network management and service provisioning via network function virtualization (NFV) and multi-access edge computing (MEC) are the key enablers to support demanding use cases in 5G networks. An early 5G deployment architecture named non-standalone (NSA) NR was proposed by 3GPP- Rel. 15 in 2017 that can fulfil the urgent deployment requirements by mobile operators, in which a device can connect to both 4G and 5G networks. To exploit the full potential of 5G, standalone (SA) NR architecture was then proposed, which is a new radio system complemented by a new 5G core network (5GC).

In general, there are five network architectures and the potential migration paths that are proposed to 3GPP- Rel. 15 as illustrated in Figure 1. Please note that this architecture can be updated in future releases.

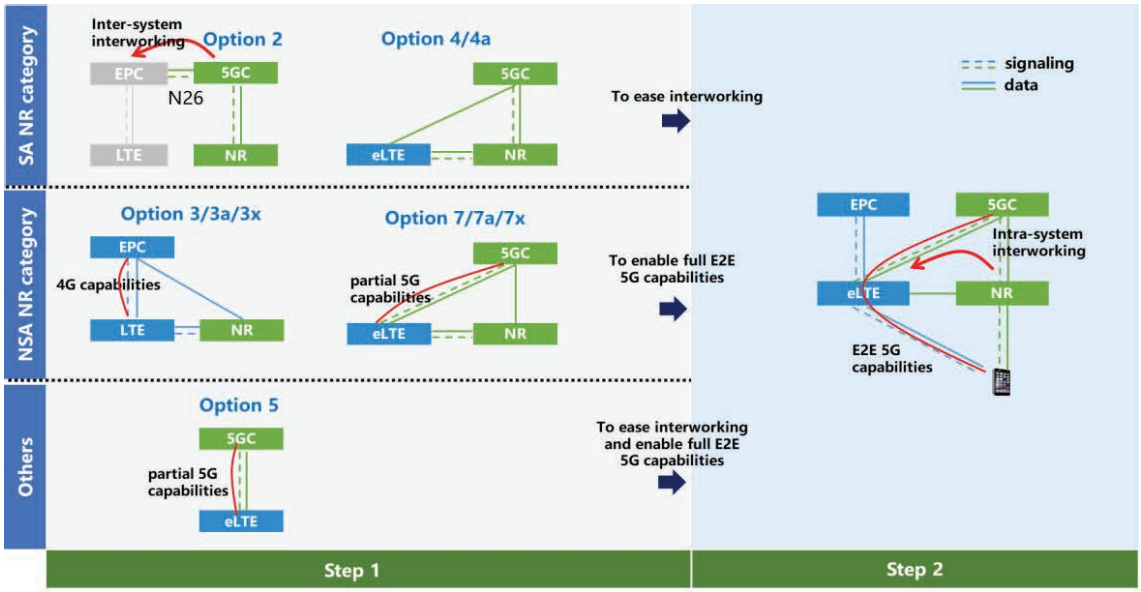

Figure 1: Five network architecture proposed to 3GPP [2].

1.2. Standardization activities towards 5G NR

Standardization refers to the definition of fundamental aspects of a mobile communications system, such as interfaces and protocols that allow different components to communicate with each other. In the field of mobile communications, the 3GPP generates the initial specifications and reports in partnership with telecommunications standard development organizations (ARIB, ATIS, CCSA, ETSI, TSDSI, TTA, TTC), referred to as “Organizational Partners.” The 3GPP covers cellular communications technologies, such as radio access, core networks, and service capabilities, and provides a comprehensive description of mobile telecommunications systems. Non-radio access to the core network and interworking with non-3GPP networks are also covered by the 3GPP specifications. In 3GPP, the Technical Specification Groups (TSG) are Radio Access Networks (RAN), Services & Systems Aspects (SA), and Core Network & Terminals (CT) [3].

Two phases have been defined towards the standardization of 5G. The goal of the first phase was to finalize basic standards for deployments in 2020 [4]. In Release 15, the first phase was completed in June 2018. The second phase included more functions that support additional services, scenarios, and considerably higher frequency bands. In Release 16, the second phase was completed in June 2020. Releases 16 and 17 are expected to play a key role for improving the applicability and availability of 5G New Radio (NR) in the near future. In Release 16, Multiple-Input, Multiple-Output (MIMO) processing and beamforming enhancements, dynamic spectrum sharing (DSS), dual connectivity (DC), carrier aggregation (CA), and user equipment (UE) power efficiency are the most prominent upgrades to the existing features. The 3GPP-approved work items in December 2019 will result in new capabilities for the three primary use case scenarios: Enhanced Mobile Broadband (eMBB), Ultra-Reliable Low-Latency Communication (URLLC), and Massive Machine Type Communications (mMTC). The goal is to accommodate predicted increases in mobile data traffic while also adapting NR for use cases in automotive, logistics, public safety, media, and manufacturing. Existing feature upgrades in Release 17 will be for functionality that has already been deployed in real NR networks or will address specific new market requirements [5].

2. Background on Technologies Relevant to the Project

In this section, an overview of technologies relevant to WP1 objectives and the respective KPIs used to quantify their performance are given. Section 2.1 presents multi-GHz communications i.e., the expansion of the frequency bands that are used in 5G as compared to previous generations, and in this perspective, section 2.2 briefly discusses millimeter-wave communications. In terms of multipath exploitation, massive MIMO is introduced in section 2.3 as a feature of 5G, and further expansions of massive MIMO that could potentially be adopted in beyond 5G communications are overviewed in section 2.4. Additionally, sections 2.5 and 2.6 present the different frame structure that is adopted in 5G NR, while section 2.7 briefly discusses non-orthogonal multiple access technology.

2.1. Multi-GHz communications

One of the most important features of new radio (NR) is the significant increase in the range of spectrum in the radio access technology. Unlike 3GPP Long Term Evolution (LTE) that supports licensed and unlicensed spectrum bands at 3.5 GHz and 5 GHz respectively, 3GPP has concluded that NR will provide operation from below 1 GHz up to 52.6 GHz in both licensed and unlicensed spectrum bands [6]. More spectrum is essential when increased network capacity and connectivity are required. Additionally, by utilizing increased spectrum, mobile networks have improved their quality of service (QoS). 5G networks aim to support a wide variety of services including, e.g., enhanced mobile broadband (eMBB), massive machine type communication (mMTC), and ultra-reliability and low latency Communication (URLLC). To support these different services, 5G will probably use higher spectrum bands, such as the millimeter-wave band, which has a lot of potential capacity.

Over the past years, millimeter wave (mmWave) communication has gained considerable attention from industry and academia because of the huge bandwidth. The mmWave bands generally correspond to frequencies from 30GHz to 300GHz. mmWave communications have some advantages compared to existing wireless communication techniques such as much higher bandwidths, small element sizes, and narrow beams. However, due to the high carrier frequency, mmWave communications has some disadvantages compared to existing wireless techniques, such as lower output power of the transmitters, higher pathloss in multipath environments, blocking effects, larger fading due to rain, and due to the need of large numbers of antennas, the power consumption is higher [7].

Due to the very high attenuation due to oxygen absorption in the 60 GHz band, located in extremely high frequency (EHF) spectrum, it has been possible to make this band unlicensed. This has made the 60 GHz band attractive for research and innovation, and it has the potential to offer high local networks

throughput for users with low-cost hardware implementation [8]. However, the very high attenuation at 60 GHz is also a major drawback in mobile communications scenarios, since the link can easily be interrupted by even small obstacles between sender and receiver, making it restricted to line-of-sight (LOS) conditions. Also, the attenuation for lower frequencies above 10 GHz can have a significant impact on overall propagation loss [9].

Beamforming techniques are key to mitigate the propagation challenges at mmWave. However, even beamformed links leak power, and potential interference can severely limit concurrent transmissions in dense networks, such as data centers. To address this problem, 3D beamforming has been identified as a flexible wireless primitive to resolve this issue in data centers [10]. 3D beamforming was first introduced by Zhang et al. in [11], and is now regarded as a promising solution in general for mmWave communications to reduce interference footprint, appropriately avoid blocking obstacles, and construct directed beams [10].

2.2. Milli-meter wave Communications

To meet the demands for mobile data traffic, cellular networks will require much greater spectrum allocations than have ever been available before. Spectrum shortages in microwave bands have motivated the use of new frequency bands for cellular communication. Large bandwidth, available in mmWave frequencies from 30-300 GHz, can be exploited for cellular communication and make them an attractive solution for 5G networks. Moreover, due to the small wavelength of mmWave signals as well as recent advances in radio-frequency circuits, it is possible to place very large antenna arrays in small dimensions and high beamforming gain can be acquired to compensate for large path loss. Therefore, mmWave can meet the requirement for 5G capacity with orders of magnitude greater spectrum and further gains from massive antenna arrays [12], [13].

2.3. Massive MIMO

Massive multiple-input-multiple-output (MIMO) is one of the key enablers of fifth-generation cellular networks. In this physical-layer technology, a base station (BS) equipped with a very large number of antennas transmit to many users at the same time and on the same frequency band. By obtaining the power gain of large antenna arrays provided by massive MIMO, the throughput of cellular systems can be drastically improved without shrinking cell size or consuming extra bandwidth. Massive MIMO and mmWave massive MIMO are main enhancements in release 16 of 5G NR [14], [15], [16] .

2.4. Distributed MIMO and Cell-Free mMIMO

As discussed in section 2.3, MIMO technology has been a great addition to the physical layer technologies that enables an increase in wireless link capacity

by using multiple transmit and receive antennas. 5G supports mMIMO technology (transmit antennas outnumber the users by an order of magnitude) and as a result has great improvements in capacity, throughput, and spectral efficiency (SE) when compared with 4G [17]. To further exploit the advantage of having multiple antennas at the transmitter researchers have suggested the use of D-MIMO, i.e., a concept where the antennas that each BS has, can be distributed in the area that it covers, improving spatial diversity at the cost of a more complex implementation that makes the analysis and implementation challenging.

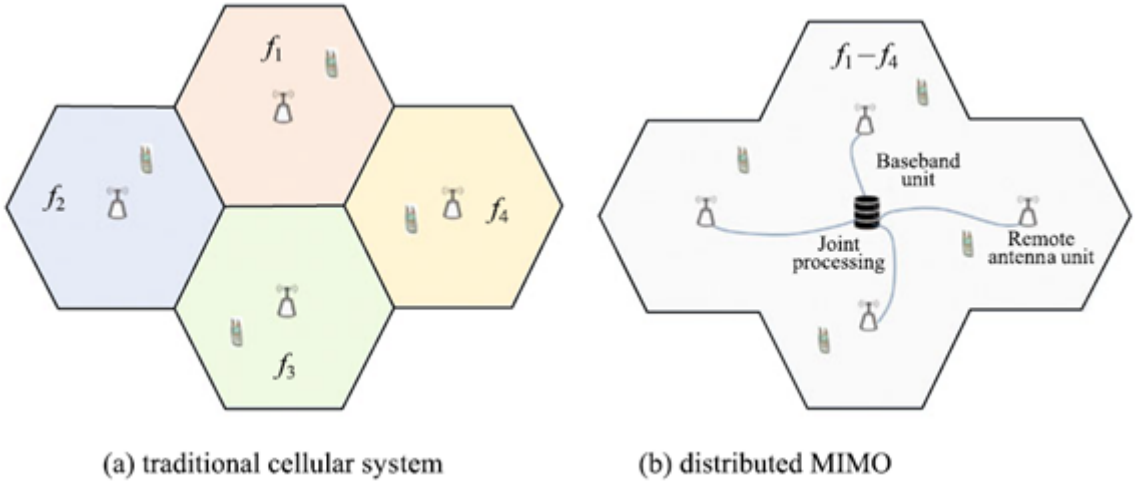

Figure 2: Traditional vs Distributed MIMO [18]

In Figure 2, subfigure (a) a traditional cellular system is depicted, where the covered area is separated in cells (or sectors) and each cell is served by one BS. In subfigure (b) a D-MIMO concept is depicted, in which a baseband unit (BBU) performs joint processing for all remote antenna units (RAU) that are connected to it and serve the same area.

The same holds for the CF mMIMO concept, where the user can be served by more than one BS, since the BS deployment is becoming denser and the cell boundaries become irrelevant, practically moving to a cell-less deployment, hence the name Cell-free massive MIMO.

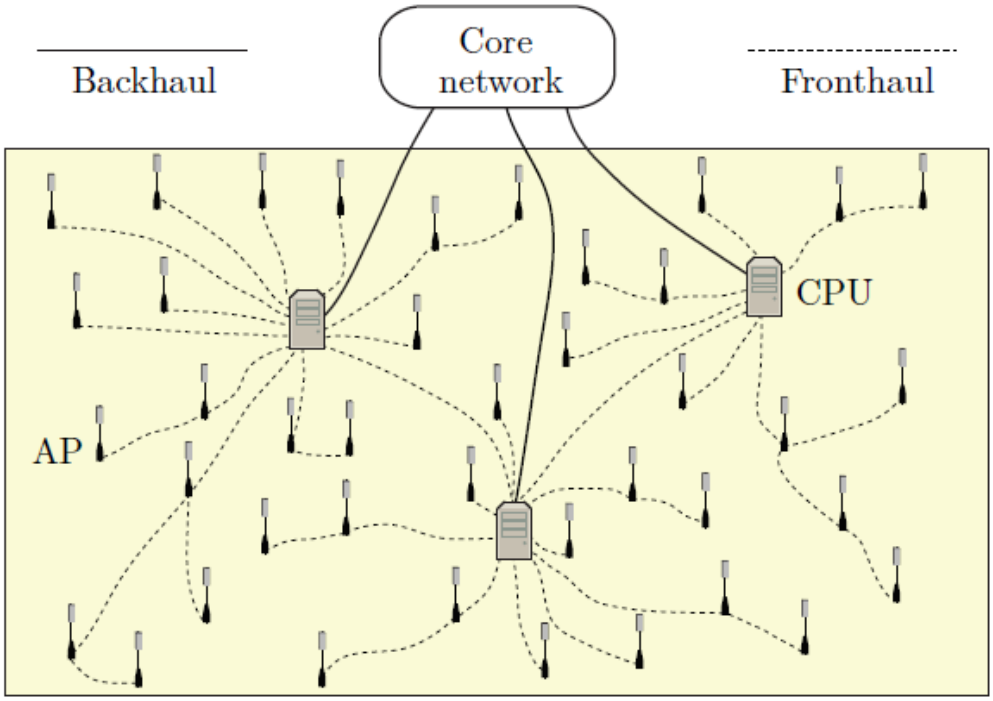

Figure 3: Cell Free massive MIMO concept [19]

Figure 3 depicts the concept of CF mMIMO, where a central processing unit (CPU) is connected to many APs that cover a geographical area with no cell boundaries.
To this extend, Ericsson has showcased an implementation of this distributed concept, particularly interesting for cases where users are concentrated in space, as in stadiums, concert halls etc, as discussed in their press release [20]. Yet, distributed MIMO concepts remain unstandardized, and ongoing work in the domain is expected to make it a beyond 5G practical technology.

2.5. Multiple numerologies

One of the interesting features of 5G NR, is that for the first time multiple numerologies is supported [21] contrary to its predecessor, the 4G RAT, i.e., long term evolution (LTE). Although the radioframe duration remains the same in 5G NR as the 4G RAT, i.e., LTE (10 ms) and is divided to 10 subframes of 1 ms each, the varying subcarrier spacing (SCS) in the interval of 15-480 KHz allows for varying number of slots (1-16 slots) per subframe. In the standards, numerologies are defined by the 15 KHz· 2^{μ} rule, where μ defines the numerology. Since each slot can contain up to 14 OFDM symbols, it is apparent that as the SCS gets wider, the slot duration gets smaller. This holds true because the SCS is the reciprocal of the OFDM symbol duration (i.e., $\Delta f = \frac{1}{T}$), with T being the symbol duration. Wider SCSs will allow fast transmissions in terms of latency and therefore will contribute to latency reduction [22] [23].

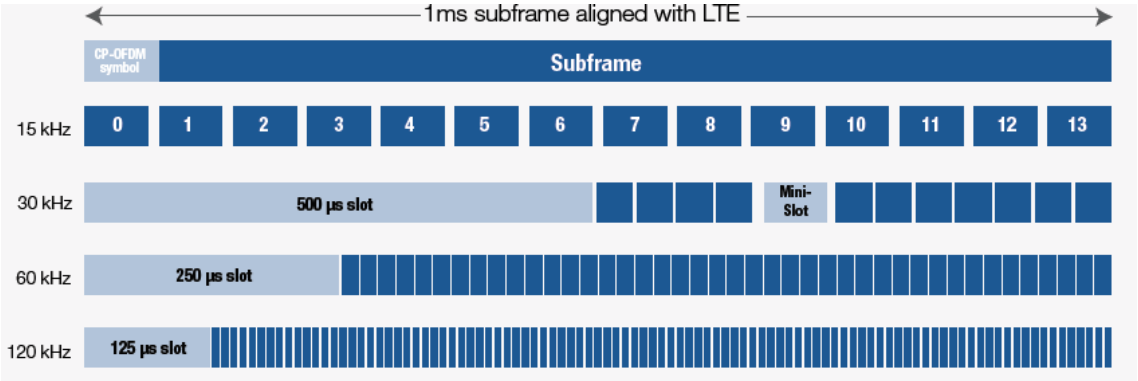

Figure 4: Multiple numerologies and frame structure [22]

Figure 4 shows a graphic representation of the different slot durations under different numerologies supported by 5G NR. Obviously, supporting different numerologies allows for greater flexibility in the frame structure, a feature that will be exploited when supporting services with diverse constraints in terms of latency. To be more precise, as 5G will also support mmWave communications, two frequency ranges (FR) are defined in the standards, i.e., FR1 (low frequency range) and FR2 (mmWave) and numerologies are tailored to them, as low SCSs will be used for FR1 and the higher SCSs are defined for use in the FR2, allowing for lower latency (shorter slot duration) and improved quality of service (QoS) as higher SCSs can better handle the Doppler effect, i.e., the inter-carrier-interference.

2.6. Mini-slots and self-contained integrated subframes

In 5G NR, two “modes” of scheduling are introduced; slot based, and non-slot based. A *non-slot* or *mini-slot* is a unit shorter than a slot (the smallest schedulable unit of time). According to 3GPP in [24] [25] a mini-slot can have a length from 1 or 2 (depending on the frequency band) to *slot-1* symbols. A mini-slot can be located anywhere within a slot. Following slot-based scheduling, slots are assigned to User Equipments (UEs), which means that scheduling is restricted to slot boundaries. On the contrary, a mini-slot is not anchored to them, since it can exist anywhere within a slot which brings more flexibility in time domain assignments, as for example in the case of latency restricted services, a mini-slot will be directly scheduled, even within an already scheduled slot, upon arrival to the BS scheduler. This approach of pre-emptive scheduling can have an effect on non-latency restricted services since their users might experience a performance degradation. An additional approach is to reserve resources specifically for latency restricted services, but it is considered less efficient as there might be cases with low traffic of low-latency services where the reserved resources remain unused.

The mini-slot structure can support very low latency. A mini-slot is not required to be aligned with the slot boundaries, so once traffic arrives at L1 it can be transmitted almost immediately (the waiting time for the next slot is skipped) and therefore the latency of this procedure is reduced. Front-load Demodulation

Reference Signal (DMRS) in mini-slots enables performing early channel estimation and it is used to estimate the radio channel for demodulation. DMRS design considers the early decoding requirement to support low-latency applications [23]. For all the above-mentioned reasons, non-slot or mini-slot is enabling low latency transmissions. Another use of mini-slots as discussed in [26] is when operating in unlicensed bands. In such a case when the channel is available for use and a contention-based access procedure is used, it is useful to *swiftly occupy* it without further delay.

Another feature that aids low latency in 5G NR is the *self-contained integrated subframe* that can be used for self-contained transmissions [27]. This setup for the subframe, allows it to contain both data and its acknowledgement (ACK) as seen in Figure 5, making therefore a transmission completed faster. Apart from low latency, self-contained integrated subframes allow for further future-proofing 5G NR as they give additional flexibility for possible future 5G services. Additionally, self-contained integrated subframes aid in the realization of advanced transmission techniques that use MIMO as they allow for quick link quality evaluation that in turn will further aid beamforming corrections especially in time-division duplexing (TDD) systems where channel reciprocity can be exploited.

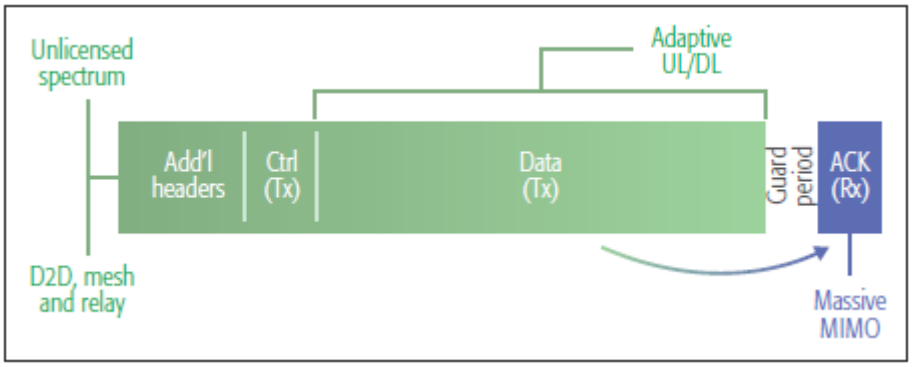

Figure 5: Self-contained integrated subframe (TDD, DL) [27]

2.7. NOMA design and waveforms

Non-orthogonal multiple access (NOMA) is an interesting technique since it enables multiple access of many users in the same resource, and generally, is divided into two main classes: power-domain and code-domain [28]. Power-domain NOMA exploits situations where the users have different power levels. As Figure 6 illustrates, in power-domain NOMA, the users nearer to the base station (BS) have better channel conditions compared to distant users who require higher transmission power to mitigate the higher path loss. The idea behind power-domain NOMA is that the users nearer the BS can employ successive interference cancelation (SIC) to remove the strong signal destined for the remote users before decoding their own signal [29].

In code-domain NOMA, random Gaussian codes are used at the transmitter in order to maximize the users' detection probability and to minimize symbol error rates [30].

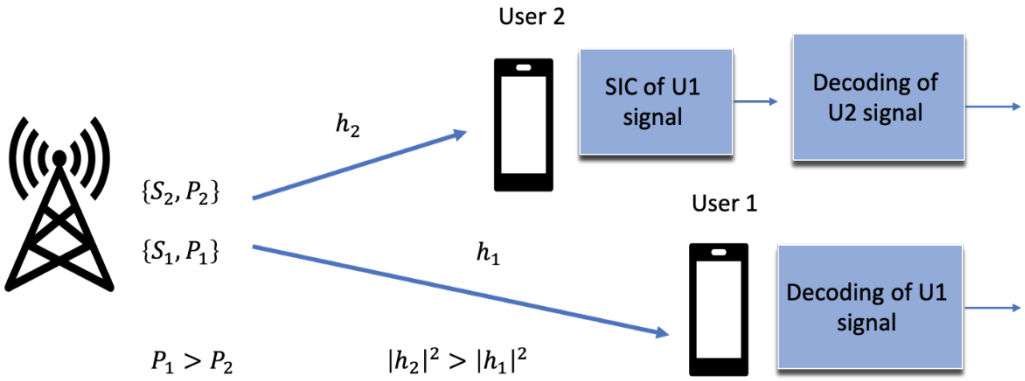

Figure 6: Illustration of Power Domain NOMA.

As Figure 7 shows, NOMA is different from the traditional orthogonal multiple access (OMA) technique. In OMA users are allocated to orthogonal resources, which means that the users have separate time slots and separate frequency allocation. In NOMA, the users use shared time and frequency slots. The superiority of NOMA over conventional OMA techniques is derived from the improved spectral efficiency due to the sharing of time/frequency/space/code resources, its allocation of different QoS levels to users based on power level allocation, and the fact that it supports massive connectivity, lower latency and an enhanced cell-edge user experience [31]. NOMA technology has been combined with other technologies such as massive MIMO [32], cognitive communication [33], physical layer security [34], network slicing, and integrated access and backhaul (IAB).

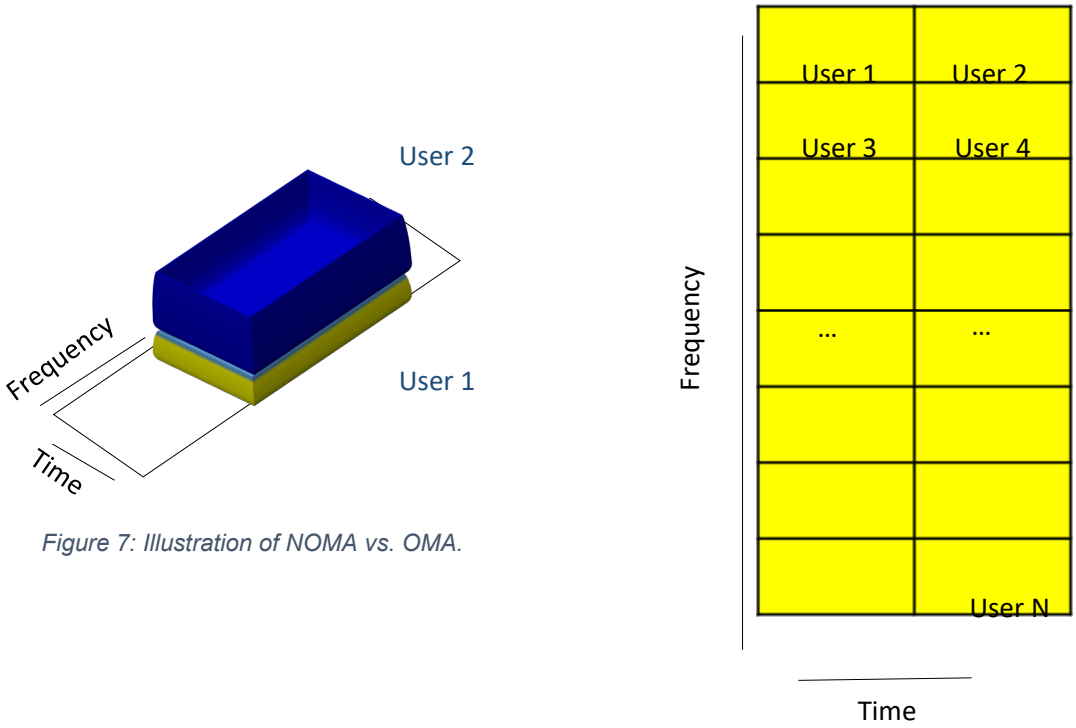

Figure 7: Illustration of NOMA vs. OMA.

3. State-of-the-art Solutions and KPIs

In this section, a thorough literature review of topics, approaches, solutions and potential open challenges are provided. The literature review topics are aligned with the scope of WP1, as publications reviewed in this section are correlated to the two research challenges WP1 aims to address, i.e.,

Challenge A1: “Spectrum and system coexistence aspects for 5G NR operation in multi-GHz bands”

Challenge A2: “5G NR forward-compatible design and future proof enhancements”.

To this extend, section 3.1 presents channel estimation techniques for mm-Wave communication systems (challenge A1), section 3.2 discusses concepts related to distributed MIMO/mMIMO as well as the use of stochastic geometry for performance analysis evaluations of such concepts (challenge A2), and section 3.3 overviews state of the art NOMA research (challenge A2).

3.1. Channel estimation techniques for mmWave bands using massive MIMO

Channel estimation is a pivotal physical layer processing block of any communication system. In particular, the performance gain provided by a communication link strongly depends on the quality of the estimated channel. Due to random scatters, reflectors, etc. in the environment, the wireless channel is unpredictable which makes channel estimation a challenging problem.

Historically, the channel estimation problem has been thoroughly studied and several traditional schemes like least square (LS), minimum mean squared error (MMSE), etc. have been proposed [35], [36], [37]. In general, channel estimation techniques can be divided into three different groups: (a) pilot-based channel estimation (b) blind channel estimation (c) semi-blind channel estimation. In pilot-based schemes, several predefined symbols that are both known at the transmitter and the receiver are employed for estimating channels, while blind techniques do not exploit the knowledge of pilot symbols and focus on deterministic or stochastic properties of the channels. Semi-blind approaches use a combination of the pilot-based and blind schemes, that is, they utilize both pilot and payload data symbols for channel estimation. Since pilot-based algorithms can result in much more accurate channel estimates compared to blind and semi-blind channel estimation, practical systems employ former approaches to acquire channel estimates. For this reason, in the following, we focus only on pilot-based schemes.

Below, we first discuss challenges with channel estimation in massive MIMO systems, both in general and specifically for mmWave systems, then we survey the literature on deep learning-based mmWave massive MIMO channel

estimation, and channel estimation in intelligent reflecting surface (IRS)-aided communication.

3.1.1. Challenges in massive MIMO channel estimation

With the advent of every generation of cellular networks, novel techniques are used to boost the performance of the last generation, but they also bring new challenges for different blocks of communication systems including channel estimation. As discussed earlier in Section 2.3, one of the main physical layer enhancements of 5G networks is massive MIMO. Massive MIMO channel estimation is a challenging problem due to the following critical problems.

i. *High pilot overhead*: Because of the large antenna array, estimating channels between transmit and receive antennas requires many more pilots than for small antenna arrays, thus increasing the overhead in the communication system at the expense of data throughput.
ii. *Pilot contamination*: To reduce the pilot overhead introduced by massive MIMO systems, one approach is reusing pilot codebooks across different cells, which causes interference between received pilot symbols using the same pilot codebook, known as pilot contamination [38].
iii. *High computational complexity*: Due to the large channel matrix in massive MIMO systems, estimating the whole channel matrix requires quite heavy computational complexity. Therefore, the implementation of channel estimation algorithms is prohibitive in practice.
iv. *FDD massive MIMO*: In frequency division duplexing (FDD) massive MIMO systems, the acquisition of downlink channel state information (CSI) at the BS is a very challenging task due to the overwhelming overheads required for downlink training and uplink feedback [39], [40]. Enabling practical implementation of FDD massive MIMO systems is a critical challenge for 5G networks.

Besides, massive MIMO systems operating at mmWave frequencies bring about novel challenges in addition to the aforementioned ones as follows.

i. *Hybrid precoding*: To reduce power consumption and hardware complexity of mmWave massive MIMO systems, one approach is employing hybrid precoding which combines analog and digital precoding [41]. Due to the limited number of RF chains in such a hardware architecture channel estimation requires new considerations.
ii. *One-bit ADCs*: Another approach for reducing power consumption and hardware complexity is using low-resolution analog to digital converters (ADCs) like one-bit ADCs [42]. However, such a hardware limitation makes the received pilot signal distorted and lowers channel estimation performance.

iii. *Beamspace mmWave massive MIMO*: Employing a lens antenna array is a new antenna architecture that requires fewer RF chains and is a promising solution that can lower the high costs of hardware and high power consumption of massive MIMO arrays [43]. The beamspace channel model and related channel estimation techniques are not well-understood, thus require further research efforts.

3.1.2. Deep learning-based (mmWave) massive MIMO channel estimation

Deep learning or deep neural network (DNN) is a specific subfield of machine learning that has shown its overwhelming privilege for solving a remarkably broad range of tasks such as computer vision, speech recognition, and autonomous car driving [44]. Owing to the versatility of deep learning, it has been recently applied to wireless communication either in a block-structured way or end-to end scenario [45]. Optimizing traditional processing blocks such as channel estimation, precoding, signal detection, CSI feedback, etc. with DNN have been investigated in the research community. In addition, end-to-end learning approaches that treat the entire communication system as an end-to-end reconstruction task have been investigated. In particular, based on the data-driven methods, the transmitter learns to encode the source data into encoded symbols (or transmit signals) to be transmitted over the cannel, while the receiver learns to recover the source data from the received signals. In the following, we briefly present the key ideas in the literature addressing the above challenges in channel estimation problems using deep learning.

In [46], a deep learning-based joint channel estimation and signal detection was first introduced, where a five layer fully connected DNN is employed as an orthogonal frequency division multiplexing (OFDM) receiver. By feeding pilot and payload received signals as input to the DNN, it is trained to reconstruct the transmitted signal without explicit channel estimation. In [47], mmWave massive MIMO-OFDM channel estimation is studied, and by exploiting time-frequency-spatial correlation, several deep convolutional neural networks (CNNs) are proposed. Furthermore, a reduced pilot overhead scheme is considered, where channels in several successive coherence intervals are grouped and estimated by a channel estimation unit with memory.

A denoising scheme in conjunction with an LS channel estimator is utilized in [48] for massive MIMO-OFDM systems that are robust to pilot contamination. More precisely, a specially designed DNN similar to the deep image prior [49] is first employed for denoising the received pilot signal and then the denoised signal is considered as the input for the LS estimator. Moreover, it is mathematically proved that the proposed channel estimation technique can achieve the MMSE performance as the product of the number of antennas, subcarriers, and coherence time interval becomes large. In [50], the time-frequency channel response in OFDM systems is treated as a 2-D noisy image and then by using

image processing techniques like super-resolution and image restoration, the OFDM channel is obtained.

Channel estimation for massive MIMO with one-bit ADCs is studied in [51]. In this paper, prior channel observation and deep learning are utilized to approximate a mapping from the received quantized signal and the true channel between massive MIMO BS and single-antenna user. It is experimentally and analytically proved that with the sufficient length and structure of the pilot sequence as the number of antennas increases, fewer pilots are needed for channel estimation, thus lowering pilot overhead for massive MIMO channel estimation. The authors in [52] consider a convolutional blind denoising network for mmWave massive MIMO channel estimation that has a robust performance for a wide range of signal-to-noise ratios (SNRs).

A new concept of mapping channels in space and frequency is proposed in [53]. Leveraging this mapping can significantly reduce pilot or feedback overhead at both co-located and distributed massive MIMO systems in the time division duplexing (TDD) and FDD scenario. Authors in [54] have revealed a deterministic uplink-downlink mapping for a wireless environment where position-channel mapping is bijective. Then, the downlink channel is predicted based on the uplink channel using a sparse complex DNN. This uplink-downlink mapping can reduce feedback overhead in FDD massive MIMO systems. In [55], an auto-encoder is employed to reduce feedback overhead in FDD massive MIMO systems. In particular, a deep learning-based encoder is used to compress the estimated channel at the receiver and a deep learning-based decoder is employed for reconstructing the channel at the transmitter. Therefore, less resources will be consumed to the feedback channel from one side of the transmission to another side.

A low pilot overhead channel estimation approach for massive MIMO systems is studied in [56]. In this scheme, a two-layer neural network is first employed to estimate the channel from the received pilot signal and then an iterative deep learning-based channel estimation and data detection scheme is considered that further refines channel estimation performance by considering detected data as pilot symbols. A deep learning approach for channel calibration between uplink and downlink in massive MIMO systems is proposed in [57]. It is shown that DNNs can learn the mapping between downlink and uplink channels with nonlinear hardware impairments and they outperform conventional channel calibration schemes.

3.1.3. Channel Estimation in IRS-aided communication

Current key enabling wireless communication technologies such as massive MIMO, mmWave communications, ultra-dense networks, etc., have significantly improved throughput and can provide the required demands for high data rate and system reliability [1]. Nonetheless, the main drawbacks of state-of-the-art implementation of wireless technologies are high power consumption and

hardware complexity which hinders the practical deployment of them. Besides, performance gains offered by current technologies can be hindered by the unfavorable wireless environment, e.g., blockage between transmitter and receiver.

IRS is a new promising physical layer technology that can provide an intelligent wireless environment and more green communication [58]. IRS is considered to be comprised of large low-cost passive elements that do not need complex RF chains for sensing and processing signals, offering energy and cost-efficient communication. Furthermore, IRS can provide a supplementary link between transmitter and receiver by intelligently reflecting impinging electromagnetic waves, thus circumventing the bottleneck of unfavorable wireless propagation conditions. With the recent advances in meta-surfaces [59] real-time phase configuration of IRS can be fulfilled by a smart controller that is connected to both BS and IRS via a control link.

For substantial performance gains to be provided by IRS-aided communication requires acquiring CSI and optimizing passive beamforming. Recently, several papers have studied the problem of channel estimation and beamforming optimization in the context of IRS-aided communication [60, 61, 62, 63, 64, 65, 66, 67, 68]. We have summarized the main ideas of these papers in the following.

Authors in [60] have studied the channel estimation problem for IRS-aided multi-user communication. By utilizing the fact that the IRS-BS channel is the same for all users, a three-phase channel estimation algorithm is proposed. In [61], the channel estimation problem of user-IRS and IRS-BS channels is formulated as a sparse matrix factorization and matrix completion problem. Then, a two-stage algorithm is proposed, where the bilinear generalized approximate message passing (BiG-AMP) algorithm is employed for sparse matrix factorization, and the Riemannian manifold gradient-based algorithm is utilized for the matrix completion stage.

A novel IRS transmission protocol is proposed in [62], where adjacent passive elements of IRS are considered as a group of elements that share a common reflection coefficient, and the channel associated with each group is estimated based on the on-off scheme. Single antenna OFDM transmitter and receiver are assumed, and an iterative algorithm is employed for joint optimization of power allocation (for sub-carriers) and IRS reflection matrix. By exploiting channel sparsity of the user-IRS-BS cascaded channel, [63] investigated a compressed sensing approach for channel estimation of IRS-assisted multi-user MIMO systems.

In [64], a new IRS architecture is considered where a few randomly distributed elements of IRS have RF chains and can sense and process signals. Based on this IRS hardware architecture, authors proposed a compressed sensing and deep learning approach for IRS beamforming. The results revealed that only a few active IRS elements are required to design IRS beamforming. Two different deep neural networks are utilized in [65] for IRS passive beamforming.

Furthermore, [66] has developed unsupervised learning for RIS beamforming, where a custom loss function is considered that maximizes the absolute value of the received signal from the direct and the reflect paths.

A progressive channel estimation and IRS beamforming approach is proposed in [67], where LS channel estimation and suboptimal IRS beamforming have been applied over pilot symbols. In [68], two different pilot transmission schemes and deep neural networks are employed for estimating direct and cascaded channels between the mmWave BS and user. Nonetheless, pilot transmission schemes and non-optimal phase configuration for channel estimation lead to extremely high pilot overhead and poor performance.

3.1.3.1. System Model

In this subsection, we discuss system models for IRS-aided communications. A basic system model for IRS-aided communication between a UE and the BS is depicted in Figure 8. In this figure h_{IB}, h_{UI} and h_{UB} represent the IRS-BS channel, UE-IRS channel and UE-BS direct channel, respectively.

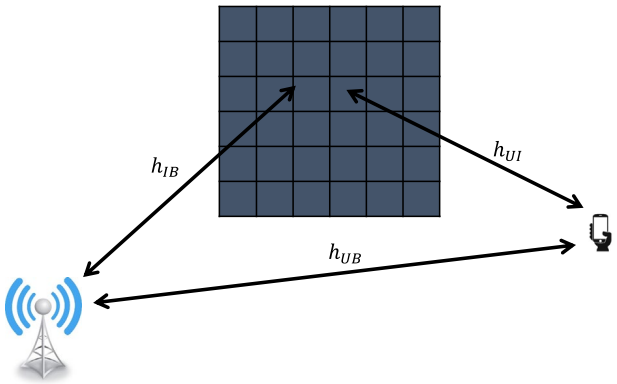

Figure 8: An IRS-aided wireless communication between BS and UE.

Different variations of this model are considered to analyze channel estimation approaches in IRS-aided wireless communication. For instance, [60], [63] have considered an uplink multi-user scenario where several single-antenna users communicate with a multi-antenna BS via both direct link and IRS-created link.

Authors in [61] assumed an IRS-assisted massive MIMO system with a single user and the direct link between BS and user is neglected as it can be estimated by traditional channel estimation algorithms, or it has been blocked and has a negligible power in the received signal. A single-antenna user and BS, and an IRS with *N* passive elements are considered for the channel estimation problem in [62]. A novel pilot transmission protocol is proposed in which adjacent passive elements share the same channel response. In particular, IRS elements are divided into several group and channel estimation is performed in these groups rather than for all the IRS elements. A similar system model is considered in [64] and the only difference is the structure of IRS in which IRS is comprised of both active and passive elements. Passive beamforming optimization is analyzed in [65, 66, 67] with a single-antenna user, BS with *M* antenna elements and IRS with *N* passive elements. Authors in [68] analyzed mmWave massive MIMO channel estimation in which a mmWave BS communicate with a single-antenna user via both the direct and IRS-reflected link.

The most important assumption in the system model for the IRS channel estimation problem is the channel model. In general, the channel model that is mainly considered for IRS-aided channel estimation is either geometry-based models or correlation-based models. For example, [61], [63, 64, 65], [68] assume geometry-based channel models where the BS is equipped with a uniform linear array (ULA) and the IRS is either equipped with ULA or a uniform planar array (UPA) and angle of arrival/departure is distributed as a uniform random distribution. However, in [60] and [67] a correlated Rayleigh fading model is assumed to capture the correlation within the antenna arrays at the BS and the passive elements of the IRS, and in [62] a simple independent Rayleigh fading model is considered.

3.1.3.2. Methodologies and Algorithms

Different state-of-the-art methodologies and algorithms are utilized to tackle the problem of channel estimation in the literature. Authors in [60] exploit the fact that the IRS-BS channel is same for all users in a multi-user scenario and proposed a three-stage algorithm that are similar to the LS approach for the uplink channel estimation. A sparse matrix factorization (BiG-AMP) and matrix completion (JBF-MC) method is used in [61] to estimate IRS-BS and UE-IRS channel. LS approach is adopted in [62], [67] to estimate the channel and [62] also propose several optimization techniques like successive convex approximation to derive reflection coefficients of IRS elements. Channel estimation problem in IRS-aided multi-user MIMO systems is formulated into a sparse channel matrix recovery problem in [63] using compressed sensing techniques like simultaneous orthogonal matching pursuit. Based on a new IRS architecture in [64], a compressed sensing and deep learning approach is developed for IRS reflection optimization. DNN are utilized in [65], [66] to optimize

IRS passive beamforming, while [68] tackles the channel estimation problem using DNN.

3.1.3.3. Simulation setup, performance metrics and future remarks

The simulation setup in [60] is divided into two different cases, without or with receiver noise, and in both cases the required minimum pilot sequence length and normalized mean square error (NMSE) are compared with a benchmark scheme that is discussed in the paper.

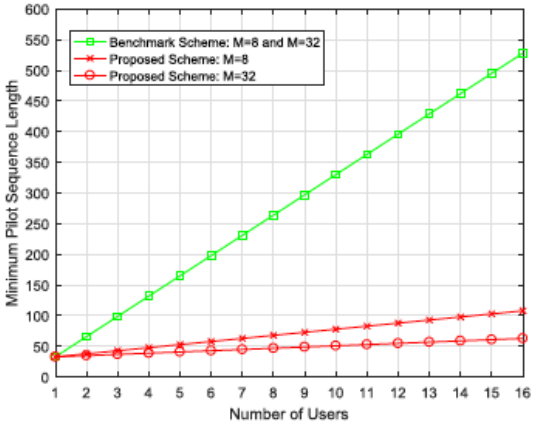

Figure 9: Minimum pilot length vs. number of users. Source: © 2020 IEEE. Reprinted, with permission, from [60].

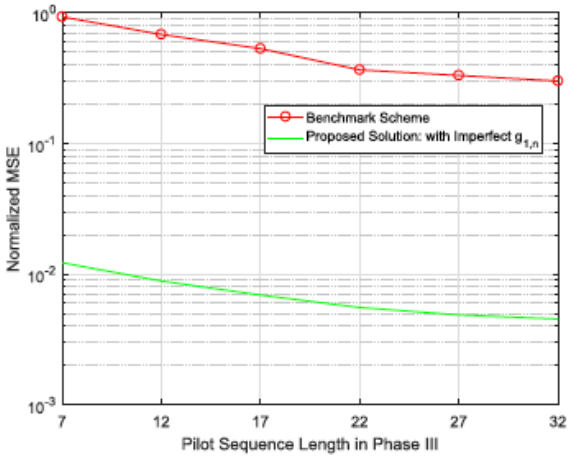

Figure 10: NMSE of the proposed algorithm in [60]. Source: © 2020 IEEE. Reprinted, with permission, from [60].

Figure 9 and Figure 10, from [60], show the minimum pilot length versus number of users and the NMSE of the proposed algorithm, respectively. As it can be seen the algorithm proposed in [60] outperform the considered benchmark in terms of NMSE and pilot overhead.

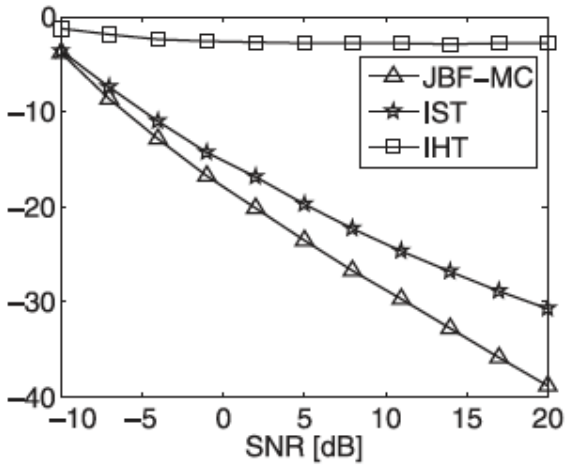

Figure 11: NMSE as a function of SNR. Source: © 2020 IEEE. Reprinted, with permission, from [61].

Authors in [61] claim that the sparse matrix factorization approach, i.e., JBF-MC algorithm has a significant performance gain over the baseline models as it is shown in Figure 11.

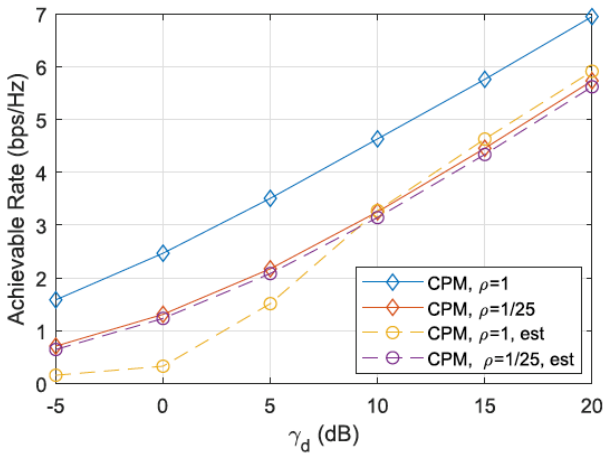

Figure 12: Achievable rate vs. SNR for different grouping ratio and perfect/estimated channel. Source: © 2002 IEEE. Reprinted, with permission, from [35].

The achievable rate from the optimized IRS beamforming in [62] is depicted in Figure 12. It is observed that the proposed Channel Power Maximization (CPM)-based method with IRS elements grouping ratio $\rho = K/M$, where K is the number of groups and M is the number of elements, is more sensitive to channel estimation error for $\rho = 1$, especially in the low-to-medium SNR regimes. As the SNR increases, the proposed channel estimation becomes more accurate and the performance gap between the achievable rate with estimated CSI and that with perfect CSI decreases for $\rho = 1$.

To sum up, the suitable performance metric for analysing proposed channel estimation performance is NMSE and for IRS passive beamforming optimization is comparing achievable rate. One crucial issue that has been overlooked in the literature is ignoring optimal IRS reflection coefficients in channel estimation stage. Consequently, the performance gain provided by IRS is not exploited for

pilot transmission which can significantly improve the efficiency of channel estimates and consequently, passive beamforming.

3.2. Distributed MIMO with analog beamforming and self-contained transmissions

This section discusses D-MIMO, Network MIMO, CF mMIMO/user-centric approaches for the physical layer in 5G and beyond 5G communication systems (Section 3.2.1) as there is a lot of research interest both from industry and academia in studying these concepts, their limitations and potential for adoption in future standards. Additionally, modelling and analysis via stochastic geometry (SG) of such technologies are presented in Section 3.2.2 as there is an increasing body of research that employs SG for such purposes of distributed MIMO techniques proving it to be a useful mathematical tool for performance evaluation. More specifically, the concepts are presented in terms of feasibility, gains and shortcomings as candidate technologies for beyond 5G mobile communication systems. A review of the relevant literature is given in the following subsections.

3.2.1. Network MIMO/D-MIMO and CF mMIMO

In this section the concepts of Network MIMO, D-MIMO and CF mMIMO systems is presented by reviewing 4 selected representative publications.

3.2.1.1. Enhancing the cellular downlink capacity via co-processing at the transmitting end

Overview: In [69], the authors suggest a co-processing mode of operation that is now referred to as Network MIMO. They refer specifically to the downlink case, where they identify the problem of inter-cell interference (ICI), i.e., a user might receive signals aimed at users in neighbouring cells. In a “traditional” cellular network such signals would be treated as interference. In their approach they assume cooperation among the serving access points (APs) and knowledge of the channel state information (CSI) between each AP and receiving user. In that way the complexity of the implementation is maintained at feasible levels. They show that under this scheme, they can achieve an average rate that is close to optimum joint processing of the received signals.
System Model: They assume a central controller that has knowledge of the local CSI, N cells and N distributed APs and an average power constraint to the system. For the APs, at most 2 of them can interfere with each user. Non-fading and flat fading channels are used.
Methodology and KPIs: They apply a linear transformation (LQ factorization) to the transfer matrix H that contains the channel gain coefficients as pre-processing along with an encoding scheme. They calculate the *achievable rate* for the typical user, as well as the *average rate over all users* and they compare it with the average rate when joint processing is not considered.

Results: Under the assumption that at most 2 adjacent APs can interfere with each user they show by numerical results and Monte Carlo simulations that the scheme they proposed outperforms the conventional approach with exception at the low SNR region both in fading and non-fading scenarios.
Advantages/Disadvantages: The main advantage of this approach is that the computational complexity is at the BS while keeping the UEs complexity as low as possible. An assumption made in this paper is a single user per cell that should be generalized as it is not practical. The authors note that more general transformations could also be used for the pre-processing with further gains.

3.2.1.2. Cooperative distributed antenna systems for mobile communications

Overview: In [70], the authors give a tutorial in distributed antenna systems (DAS). The main motivator for deploying DAS is to improve the cell-edge user experience, although initially as a concept it was aimed at improving indoors service coverage. The basic operation of a DAS system is to serve users in a cell but instead of having all the BS antennas collocated, they are geographically distributed. In the following figure taken from [70] a graphic comparison of a DAS and a collocated antenna system (CAS) is shown.

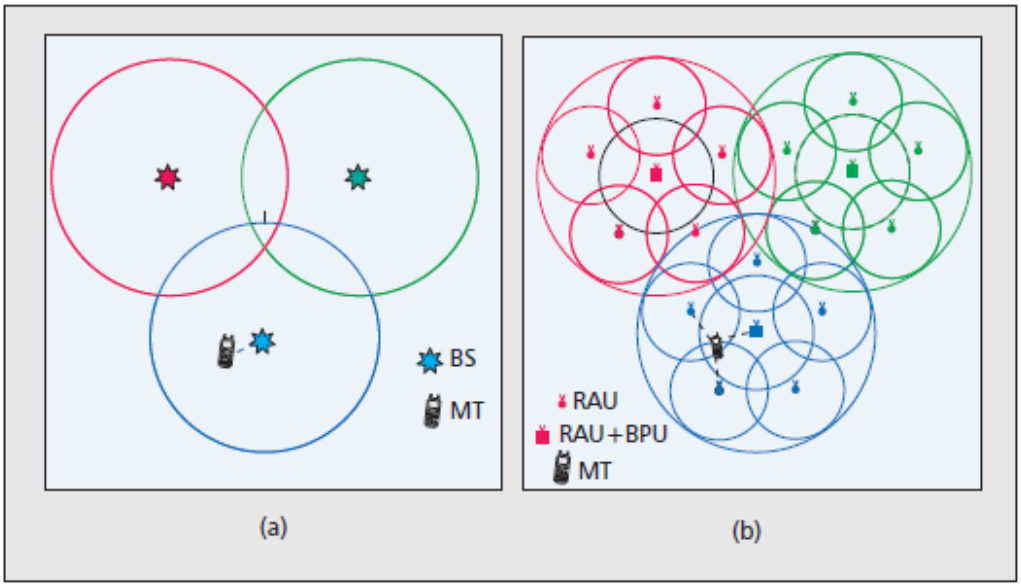

Figure 13: CAS vs DAS (cellular concepts) [70]

System Model: They define their configuration with three variables (M, L, N), where M is the number of antenna elements of each user, L is the number of antenna elements per RAU and N is the number of RAUs per DAS and $L \geq M$.
Methodology and KPIs: They give expressions for UL and DL *channel capacity*. They discuss *interference suppression* either by using precoding techniques to aid the UEs in decoding in the DL or by using joint processing with channel knowledge at the receivers. Next, they address *power allocation* strategies, where they specifically address current approaches like water filling (WF) and

equal power allocation (EPA). They find that both can be problematic as in the first case the implementation is complicated, and in the later the performance can be suboptimal. To this extend they discuss maximal path loss ratio (MPR) where the power allocation for each user is a function of the path loss it experiences. They also address the *handover process* for which an extension from the CAS approach is not optimal. They use a capacity-based handover approach for the DAS where the UE estimates the average capacity of neighbouring cells and when a larger value than the current is calculated it is reported back to the BS. The BS will decide whether to approve the handover and pass on information back to the UE.

Results: This concept was also tested with field trials in an 8 X 4 distributed MIMO setup, where the 8 transmit antennas were divided to 2 BSs, each containing 2 RAUs with 4 antenna elements while UEs were equipped with 4 antenna elements as well. Additionally, they show analytical and Monte Carlo results on the uplink capacity, outage capacity showing that the DAS is more efficient when compared to an equivalent CAS (same total power and number of antennas). They also show comparison results of WF, MPR and EPA power allocation schemes, where WF outperforms the rest, but MPR is still a good candidate. Lastly, they compare multi-user and single-user DAS and CAS setups in terms of DL average capacity per user, and they show that the DAS outperforms the CAS as expected, the single-user scenario has better average capacity than the multi-user scenario in both system setups as expected and that both systems are noise limited in low SNR regions and interference limited in high SNR regions.

Advantages: The authors deem the approach of cooperative DAS interesting due to the improvement in service coverage and the statistical independence of the signal due to geographical distribution (different fading factors) that would in turn benefit the system capacity. Intuitively, DAS yield improved results due to the following features: i) the antennas are brought closer to the users therefore improving conditions for cell-edge users, ii) the distributed antennas can be jointly exploited to improve SE via cooperation.

3.2.1.3. A new look at cell-free massive MIMO: making it practical with dynamic cooperation

Overview: In [71], the authors discuss the concept of CF mMIMO. They describe the relation between Network MIMO as a predecessor (as dynamic cooperation clusters-DCC, i.e., a concept where the user selects a subset of antennas to serve them, forming a *DCC* as seen in the following figure) and CF mMIMO as a special case. In previous CF mMIMO literature [72] [73], the solution presented was not scalable and the authors here present a scalable solution inspired by DCC, so they extend the CF concept to user-centric clustering to make it scalable (by their definition) as seen in Figure 14.

System Model: They assume a topology of a CF network with K single antenna UEs, L APs, N antennas and consider $M=LN$ antennas in total with $M >> K$. The

APs are connected to edge-cloud processors that handle the processing of coherent joint transmissions in time-division duplex (TDD) mode.

.

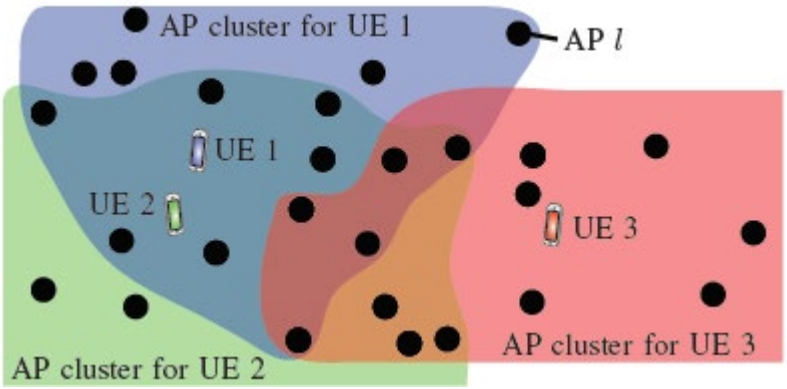

Figure 14: Dynamic cooperation clusters [71]

Methodology and KPIs: Their approach is to restrict each AP to serve at most one UE per pilot (limiting *pilot contamination,* i.e., interfering pilot signals at the AP when more than one UEs are assigned the same pilot) and only compute CSI, beamforming vectors and power coefficients for these users only. They describe a process to create the DCC for the user. They derive analytical results for the *spectral efficiency* (SE) in the DL and UL with their proposed precoding strategies.

Results and Advantages/Open Challenges: Their results show that the signal-to-leakage-an-noise (SLNR) precoding is outperforming Maximum Ratio (MR) in the DL, and its counterpart Regularized Zero-Forcing (RZF) is outperforming MR in the UL. So basically, they show that they have a scalable version of CF mMIMO as the number of users grows large, that outperforms the known performance of CF mMIMO that is not scalable. Open problems to this approach are power allocation in the DL and how to best exploit the fronthaul capacity.

3.2.1.4. Ubiquitous cell-free Massive MIMO communications

Overview: In [74], the authors describe the CF mMIMO concept through extending the mMIMO concept. Through this perspective, mMIMO is assisting greatly in improving SE and reducing ICI, but still, ICI is the limiting factor in network densification, and mMIMO cannot completely cope with it, because of its cellular architecture. So, in terms of SE, gains can be achieved with signal coprocessing at multiple APs. They attest the lack of standardization of coprocessing concepts to their inherent support of cellular architecture designs that are the *root cause of limited gains*.

Methodology & KPIs: In the DL, APs cooperate to serve UEs in a user-centric manner, abandoning the cell boundaries. In the UL, processing can happen locally at the AP, centrally at the CPU, or partially at the AP and then forwarded to the CPU. Obviously, the central approach brings more gains, but this strategy

is fronthaul-limited. In the following figure, the difference in *SE* in a cellular and a cell-less architecture is depicted.

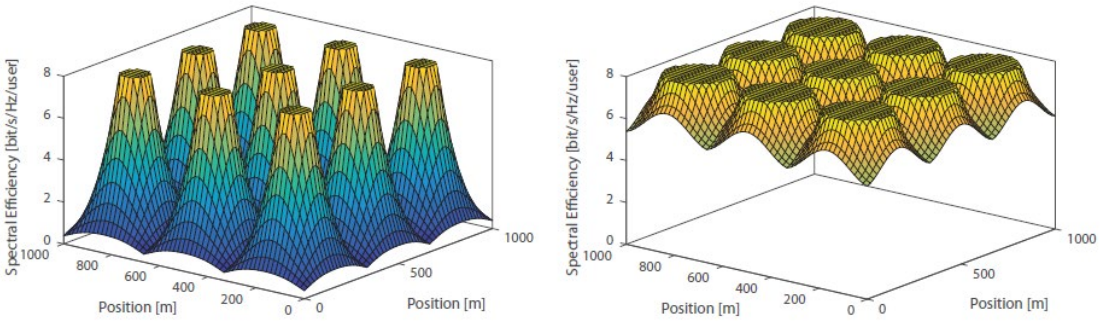

Figure 15: Cellular vs Cell-Free architecture [74]

What we see in the left part of Figure 15 is the traditional cellular concept, were users experience very low SE at the cell edge, due to interference. In the right part of Figure 15, the SE in a CF mMIMO network, where due to the abrogated cell boundaries and the cooperation, users experience better service quality (high SE) almost uniformly in the geographical region. They discuss the features of favourable propagation (i.e., having nearly mutually orthogonal channel vectors) and channel hardening (i.e., making the fading channels behave as almost deterministic) in the CF mMIMO concept indicating that the latter is weaker in the CF mMIMO architecture. In terms of duplexing, when operating in frequency-division duplex (FDD) mode, the spatial correlation of the channels may deteriorate favourable propagation (i.e., cause inter-user interference unless user subgrouping and scheduling are applied) and will require accurate channel estimation which is challenging. Therefore, TDD mode is preferable especially since we can exploit channel reciprocity. In this case, the BS would have to assign non orthogonal pilots to UEs (when the number of users is greater than the number of the length of the TDD frame in samples) thus causing pilot contamination. So, an important aspect of CF mMIMO is how to assign pilots with respect to limiting the pilot contamination phenomenon. They also address power allocation strategies for CF mMIMO, and they briefly discuss the radio stripe approach by Ericsson [20] as a practical implementation of CF mMIMO.

System Model and Results (case studies): Assuming a CF mMIMO concept with *L* single antenna geographically distributed APs serving cooperatively *K* users with *L* >> *K*. This enables the properties *of macro-diversity* and *favourable propagation.* They also present SE results under different power allocation strategies in indoor and outdoor scenarios for the radio stripes concept.

Open Challenges: Finally, they conclude with a list of open challenges for the CF mMIMO concept. More specifically they identify distributed power allocation schemes with respect to parameters as fairness, latency and throughput, distributed signal processing techniques with respect to backhauling, resource allocation policies tailored to the CF concept aided by channel modelling that is taking into account channel measurements, dedicated channel estimation

approaches, 5G and beyond standard compatibility and prototyping as research areas of interest for the CF mMIMO concept.

3.2.1.5. Comparative Study

In [69] the authors discussed Network MIMO, a concept where APs cooperatively serve users with local CSI knowledge and therefore can increase the rate of the served user. They show that the cooperative scheme outperforms conventional cellular concepts in terms of achievable rate, and in doing so they managed to keep the BS computational complexity low, but still the framework would need generalization. In [70], the authors present the cellular D-MIMO concept and outlined the way of working and the achieved gains along with their source. They discuss DAS-related techniques (power allocation, handover etc) and their benefits and shortcomings. They conclude that the DAS network architecture is a promising approach for future wireless networks, but they omit practical implementation challenges that they still face in contrast with [71]. In [71] the authors extend the concept of Network MIMO to CF mMIMO, and they show that by utilizing the DCC strategy they can create a scalable version of CF mMIMO that due to the choice of precoders can outperform current systems performance but still faces practical implementation challenges like optimizing the fronthaul capacity utilization and optimal power allocation among the users. In [74], the authors discuss the fundamental processing and practical implementation aspects of the CF mMIMO concept and discuss why they believe it is a promising concept for future networks that can be practical and scalable and list open research challenges towards its realisation.

In conclusion, the papers discussed in this section outline the problems that distributed technologies like D-MIMO and Network MIMO are facing in terms of practicality as they are both network-centric i.e., cell-based architectures, and suggest that a user-centric, i.e., cell-free concept is the way to further improve the system performance in terms of SE, EE, capacity, throughput and scalability for beyond 5G communications. To this extend, CF mMIMO as discussed in [71] [74] is a technology that combines the mMIMO operation with dense deployments and user-centric architecture, i.e., a cell-less or cell-free architecture design that is not burdened by interference problems as seen in the cellular architectures, and is scalable, but still faces open challenges like user subgrouping/scheduling, power allocation strategies, backhaul limitations and CSI acquisition that need to be addressed before it becomes a practical approach ready to be used in future wireless communication systems.

3.2.2. Stochastic geometry analysis of network MIMO and cell-free massive MIMO

In this sub-section, the use of stochastic geometry (SG) for modelling and analysing of cell-free massive MIMO systems as well as Network MIMO systems

(and cell-less approaches in general) is presented through selected representative publications on the use of SG for performance analysis.

3.2.2.1. Performance analysis of cell-free massive MIMO systems: a stochastic geometry approach

Overview: In [75], the authors evaluate the performance of a CF mMIMO system and compare it with small-cells (SCs) i.e., hotspot tier BSs.
System Model: They consider a set of Poisson point process (PPP) distributed APs with known number of antennas at the APs and known number of APs in the setup. They also assume Rayleigh independent and identically distributed (i.i.d.) small scale fading and distance dependent large scale fading for their channel model.
Methodology and KPIs: For the DL they assume TDD transmission mode, and they exploit the channel reciprocity feature where they use the channel estimates calculated in the UL through minimum mean square error (MMSE) estimation for all the users. They also consider conjugate beamforming and additive white Gaussian noise (AWGN) in their setup. Using SG, they derive expressions for the *achievable rate and coverage probability*. They then verify their analytical results with Monte Carlo simulations.
Results: They show that increasing the AP density results in higher coverage which saturates after a value and CF mMIMO outperforms the SC setup, a straightforward result, as CF mMIMO takes advantage of the cooperation among the APs in contrast with SCs, while at the same time, the massive number of antennas introduce channel hardening and favourable propagation for the CF mMIMO concept. In fact, CF mMIMO systems systematically offer higher coverage than SCs due to these features but the coverage probability decreases when the SNR threshold is increasing as the system experiences inter-cell and inter-user interference. Additionally, they show that increasing the number of supported users decreases the average achievable rate (more users translate to more interference and pilot contamination) but still CF mMIMO outperforms SCs, as joint processing is proving to be more robust in high interference scenarios. Furthermore, the training period obviously has an effect in the achievable rate, as longer training periods can reduce the pilot contamination effect making CF mMIMO systems more robust. Lastly, they note another straightforward observation, as increasing the path-loss exponent decreases the rate monotonically for both setups as far positioned users will suffer signal degradation and therefore a larger number of APs would be beneficial.
Pros/Cons: In conclusion, this paper shows that CF mMIMO is a competitive approach for designing future communication systems as it outperforms SotA concepts, but the results they show are heavily dependent on the assumption that the features of channel hardening and favourable propagation are strong. This assumption can hold when the APs are densely deployed but sufficient separation is implied.

3.2.2.2. Performance analysis for user-centric dense networks with mmWave

Overview: In [76], the authors evaluate the performance of systems operating in mmWave with a dense user-centric deployment in terms of ergodic capacity and coverage probability for which expressions are derived using SG.
System Model: They assume a virtual cell architecture where APs are distributed in a geographical area connected to a controller and only a cluster of the nearest APs to the UE are serving it (k-NN clustering).
Methodology: They assume a set of homogeneous PPP distributed APs as well as distance dependent fading and they take into account the blockage effect that is substantial in mmWave frequencies. They consider different small-scale fading distributions (i.e., Nakagami, Rayleigh, and no fading) and they also adopt a noise limited approximation. Because of the dense deployment they assumed, they also make the strong assumption of always being served by APs that are in line of sight (LoS). Lastly, they assume sectorized antennas and they take under consideration the antenna gains in their derivations. A representation of a virtual cell can be seen in the following figure.

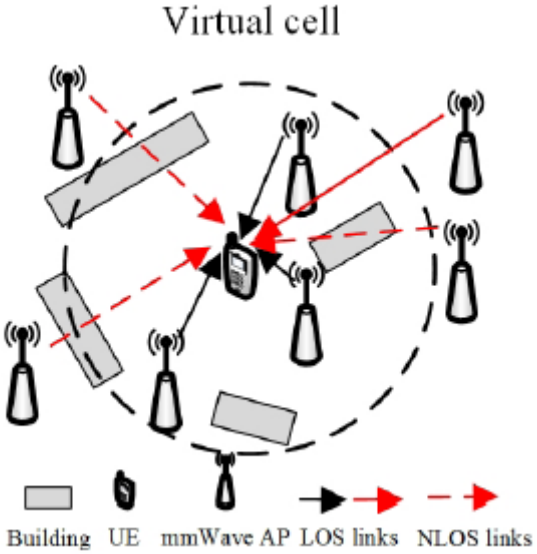

Figure 16: Virtual Cell, useful and interference links [76].

Results and KPIs: Through simulations they show that the *coverage probability* decreases with the target SNR threshold, a straightforward result as high SNR in conjunction with LoS APs translates to increased interference. They also show the straightforward result of decreasing coverage probability with the blockage parameter in all three fading scenarios. Furthermore, they show that the coverage probability is increased when cooperation is assumed for all fading scenarios. They justify their noise limited approximation by comparing results in terms of coverage with and without the assumption. In terms of capacity, they show that it increases with the blockage parameter and that is justified as more blocking has an interference limiting effect as more APs are in non-line of sight (NLoS). They show that the capacity increases when cooperation among APs is assumed but

they also show that the noise limited approximation is overestimating the *ergodic capacity* and probably this assumption should only be made for low density deployments with high blockage probability.
Pros/Cons: In conclusion, this paper shows that AP cooperation is beneficial in terms of coverage and capacity for mmWave user-centric networks, under the assumptions of LoS serving APs cluster and the noise limited approximation which is only justified for low density and high blockage scenarios.

3.2.2.3. A Stochastic Analysis of Network MIMO systems

Overview: In [77], the authors evaluate the performance of Network MIMO systems with the aid of SG tools. They use disjoint clusters to perform cooperative processing and make the strong assumption of a delay-free infinite-capacity backhaul along with perfect CSI knowledge within each cluster.
System Model: The authors take into account APs that are distributed according to a homogeneous PPP as shown in Figure 17. They consider a known number of antennas for each BS and assuming a known total power constraint, apply EPA.
Methodology and KPI: They consider fading effects in their analysis and apply zero-forcing (ZF) beamforming. Through a moment-matching technique they evaluate the signal power distribution and the interference power distribution which they use to derive the *ergodic sum-rate per BS* of a Network MIMO system.

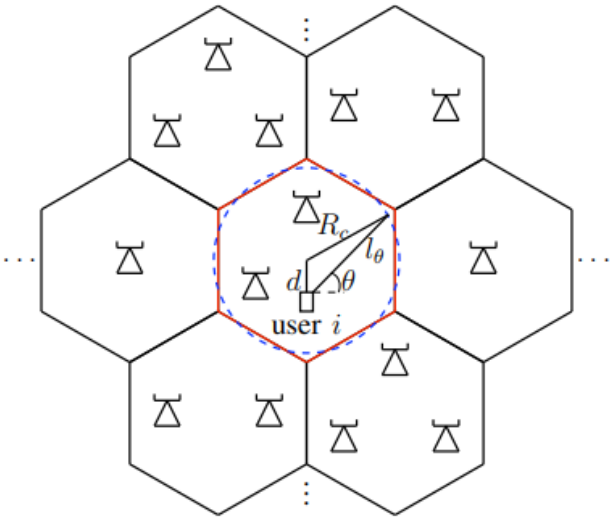

Figure 17: A clustered Network MIMO system [77].

Results: They use this to evaluate the performance of the Network MIMO system with respect to the loading factor, i.e., a ratio of the number of scheduled users and the number of BS antennas. More specifically, they evaluate the ergodic sum-rate for different values of the loading factor, and they observe that the ergodic sum-rate increases when the loading factor goes from 0.2 to 0.6, concluding that in such a system, at most 60% of the resources can be used to optimize the rate and the rest should be devoted to increasing diversity (as shown

through extensive *loading factor* vs. *ergodic sum-rate per BS* simulations). They extend this result to the use of weighted MMSE (WMMSE), where they confirm that 50%-55% maximize the ergodic sum-rate. Lastly, they study the effect of the cluster size at the ergodic sum-rate.

Next, they evaluate the ergodic sum-rate per BS in different processing scenarios. They show that isolated cells have the best ergodic sum-rate (as expected), followed by a Network MIMO system with isolated cluster, and lastly in terms of performance a clustered network MIMO system. The authors attest this is because although intra-cluster interference can be suppressed through beamforming, the same does not happen with out-of-cluster interference no matter how large the clusters are.

Pros/Cons: In conclusion, this paper showed that the cooperation gains that can potentially be obtained from a Network MIMO system are severely dependent on the loading factor of the system and fundamentally limited by the out-of-cluster interference. Network MIMO does achieve gains when compared to uncoordinated single-cell processing but cannot achieve the ergodic sum-rate of an isolated cell. Another disadvantage of this paper is the strong assumption of infinite backhaul capacity and perfect CSI knowledge within each cluster, as this is one of the most challenging aspects of Network MIMO and probably the reason why in reality this architecture does not yield the gains shown in theoretical studies.

3.2.2.4. Comparative Study

In [75], the authors compare a CF mMIMO concept with a SotA approach that deploys SCs via SG tools. They show that the CF mMIMO concept outperforms the SC architecture showing substantial gaps in the performance both in terms of coverage probability and average achievable rate, mostly due to the feature of favourable propagation and channel hardening, but also due to the cooperative processing. In [76], the authors evaluate a user centric mmWave dense network that assumes cooperation among k-NN APs to the user. They evaluate the performance in terms of coverage probability and ergodic capacity, and they show that under different fading scenarios, cooperation among the APs is beneficial proving that the user-centric approach is a desirable feature for future communications systems and verify the theoretical knowledge that traditional cellular designs bring limitations in performance due to the cell-edge effect. They show that the ergodic sum-rate per BS increases as the average number of BSs per cluster also increases. That is, larger clusters improve the ergodic sum-rate per BS although better performance is observed when the BS locations are fixed rather than PPP distributed. Also, single-cell processing approaches the disjoint cell processing scenario when the number of BSs per cluster increases. In [77], the authors evaluate the performance of Network MIMO systems with respect to the loading factor and the size of the cooperation clusters. They show that the ergodic sum-rate per BS is maximized when at most 60% of the spatial resources

are dedicated to the rate maximization and the rest should be allocated for diversity purposes. Additionally, they show that the performance in terms of average sum-rate per BS is limited by the out-of-cell interference and as there is a signal power penalty even when the cooperating clusters are impractically large. Network MIMO can yield improvements in terms of rate when compared to single cell transmissions but cannot achieve that of an isolated cell. In addition, the demands for a Network MIMO system such as near perfect CSI acquisition and distribution through backhaul links could affect the practical implementation and scalability of such a system.

In conclusion, the papers reviewed in this section have confirmed the theoretical remarks made in section 3.2.1 that underlines the technologies discussed in this section. More specifically, it is shown that cell-less deployments outperform their cellular counterparts, and additional gains can be obtained when taking advantage of their characteristics (i.e., making sure that features of mMIMO like favourable propagation and channel hardening are still present in the cell-less approach). An additional remark for the performance evaluation under SG is that care should be taken when setting parameters and making assumptions as it is shown through the results that sometimes the assumptions were too strong to hold in reality, as the SG results were not validated by simulation results or measurements as is the case in [76], where the authors make the assumption of the system being noise limited thus omitting interference, that leads to an overestimated ergodic system capacity.

3.3. Application-aware design of NOMA waveforms
Traffic models beyond 5G

In this section we discuss NOMA as a tool for next-generation wireless networks. We begin with a brief discussion of the state-of-the-art in NOMA research, then we focus on the role of MIMO in NOMA, followed by a brief introduction to network slicing. Finally, we present a specific use case of NOMA and network slicing related to the problem of forest firefighting.

3.3.1. State of the art in NOMA

Despite the various advantages of NOMA technology, there are some limitations and implementation issues that must be addressed. First, before a UE can decode its own information, it must decode the information of all other higher-powered signals [78]. A power difference between near and far users is needed to achieve the benefits of power-domain multiplexing. Another challenge is that any error in the SIC decoding will likely lead to errors in the subsequent decoding of other signals [79].

Timotheou et al. [79] investigated the optimal power allocation (PA) to maximize fairness in terms of data rate for downlink users assuming full instantaneous channel state information (CSI) and average CSI at the

transmitter. They concluded that NOMA is a promising multiple-access (MA) technique for future 5G communication systems because it can effectively achieve fairness through appropriate design of the PA. Using the outage probability, the optimal power allocation based on average channel state information (CSI) was investigated in [79]. In particular, the stochastic capacity of MIMO-NOMA systems with second order statistical (SOS) CSI at the transmitter was investigated. The majority of NOMA research assumes perfect knowledge of the CSI. The assumption of perfect CSI at the transmitter may not be accurate, because achieving perfect CSI requires a substantial amount of system overhead especially with a massive number of users. So, achieving “perfect” CSI is still challenging. Yang et al [80], are focused on the use of partial CSI to improve the spectral efficiency of NOMA, and to reduce the complexity of the system. In addition, they compare the performance of NOMA with partial CSI to NOMA with perfect CSI, and these comparisons are useful to NOMA system designers. The system model in the downlink with a single-cell is based on two different types of NOMA schemes, imperfect CSI with channel estimation error modelled with a complex Gaussian distribution, and second order statistical (SOS) CSI. The performance was investigated with respect to outage probability and average sum rate. Based on the analytical results, the conclusion is that NOMA is not robust to imperfect CSI, and in such cases, it is preferable to implement NOMA with SOS, and the two NOMA protocols can obtain better performance than conventional OMA. Ding et al. [81] studied the impact of relay selection (RS) on the performance of cooperative NOMA. They were able to show that NOMA yields a significant performance gain over OMA in terms of both diversity gain and outage probability across all possible RS schemes.

3.3.2. MIMO Aspects of NOMA

Normally in NOMA without multiple antennas, the ordering of the decoding is based on the scalar channel gains of the users. When multiple antennas are involved, the effective channel gains now depend not only the physical channel itself, but also on the beamforming vectors employed at the transmitter and receiver. This complicates the design but also provides more degrees of freedom for achieving good performance.

The use of NOMA in the MIMO downlink has typically focused on cases where the users are grouped into clusters [32], [81]. Some type of beamforming is used to differentiate the clusters, either transmit beamforming at the BS or receive beamforming at the users, and then NOMA is employed within the clusters in order to further separate the user signals. There are two main cases. In the first case, the BS does not possess CSI, and it is the users with multiple antennas that exploit CSI to eliminate the inter-cluster interference. This requires that the users have at least as many antennas as the BS. Within a cluster, the users can employ a beamformer that eliminates the signals destined for the other clusters, and then NOMA is applied by the users within the cluster. The power

control at the BS is implemented by sorting the users within each cluster according to the strength of their effective channels (combination of receive beamformer and MIMO channel). This can presumably be achieved without instantaneous CSI at the BS if at least the channel statistics are known, or if the users feedback their effective channel gains after removing the inter-cluster interference. Then within each cluster, NOMA can be applied as normal; users with strong channels perform successive interference cancellation, while users with weak channels treat the interference as noise. A problem with this general approach is that the grouping of the users into clusters is less effective when the BS does not have CSI, since a good distribution of channel quality within the clusters cannot be guaranteed. Another difficulty with this approach is that the users must have at least as many antennas as the BS, which is not a typical situation.

In the second case where the BS does possess instantaneous CSI, the assignment of the users to clusters can be made in a more intelligent way that can enhance the benefits of NOMA. For example, the users can be grouped according to those that share the same channel spatial covariance matrix. In this case, the BS can eliminate the inter-cluster interference by choosing an appropriate precoder/beamformer. This eliminates the requirement that the users must have more antennas than the BS and is the more reasonable approach particularly in massive MIMO scenarios. With appropriate power control, the users within each cluster then can implement NOMA as in the previous case [32], [81].

3.3.3. Brief Summary of Network Slicing

5G networks aim to support a wide variety of services including, e.g., eMBB, mMTC, and URLLC [82]. Achieving an appropriate throughput, latency, and reliability as well as energy- and cost-efficiency is a challenging task. A key enabler to cope with these requirements is the use of network slices. Network slicing (NS) allows the provisioning of these different services on a shared physical infrastructure. Each network slice is an end-to-end independent virtualized network which allows operators to activate different deployments using different parallel architectures.

The different applications of network slicing include smart factories and the tactile internet in which the wireless communication signals convey so called kinaesthetic information to a client in order to achieve the manipulation of remote objects [83]. The latency requirement in these applications is challenging and can be as low as 1ms in 5G and requires high reliability and security. Network slicing can address these challenges using virtualization, which allows the instantiation of network elements at suitable locations for communication. Apart from the advantages of using network slicing, mobile network operators can efficiently analyze the resulting operational cost. Based on the analysis in [83], NS also enables allocating different network resource bundles to different slices. This helps to structure resource management and make it flexible and efficient.

3.3.4. Potential use-cases for NOMA

3.3.4.1. Overall description of network slicing for forest firefighting

Climate change and the growth of the human population into previously unoccupied areas has led to an increase in the number and size of large fires [84]. These increases, and the proximity of human communities near the fires has made fighting them very difficult and risky and are putting a strain on available firefighting resources [85]. Future firefighting efforts will require advanced communications and airborne support to improve not only the ability to contain the fires, but also protect firefighting personnel. Advances in 5G communications can play a big role in filling this need, providing both intelligence about the fire environment [86] and communications support for personnel on the ground [87]. Using unmanned aerial vehicles (UAVs) together with 5G communications systems is one example of new technology that can improve wildfire detection and intervention, as well as aid firefighters in their operations. UAVs and other autonomous devices can be applied in many different ways to support firefighting operations, including detection of fire events, ignition of backfires, search and rescue, providing communications support where infrastructure does not exist, measurement of toxic gases, measuring the fire perimeter in remote areas that are otherwise unreachable, collecting visual data about the fire, etc. [88]. Figure 18 illustrates a typical firefighting scenario supported by a group of UAVs. The various components of the system are described below.

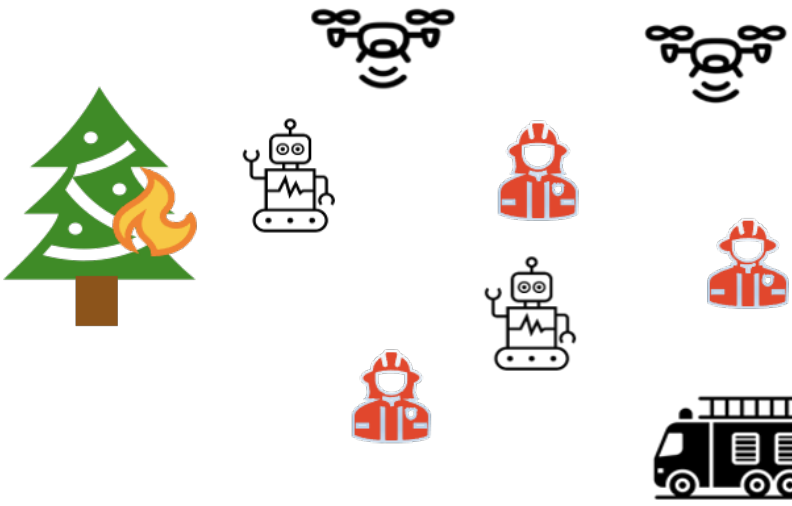

Figure 18: Illustration of actors in the firefighting scenario. Creative Commons: Drone, fire, truck, icons based on icons by Felix Westphal, Vectors Point respectively, from thenounproject.com

Robots provide support for a number of different tasks and can be used instead of humans in situations where there is significant danger. Their most important roles will be to provide information about the scene and establish communication links where they would otherwise not exist. The key to the effective use of robots is having a sufficient cadre of sensors on board that allow the robot to navigate complicated environments that possess visual obstructions such as smoke, gas and dust, physical obstructions such as barriers, trees, rocks,

etc., that limit movement, and buildings, trees, or mountains that obstruct communication or GPS signals. The robots become part of the firefighting team and play a role similar to the firefighters in protecting the team members and improving the response of the team to the disaster. Like their human counterparts, the robots must interact with each other, with human members of the team as well as the field commander and provide information as needed without being distracted.

The incident commander is the lead firefighter and is in charge of the fire response as well as the deployment of human and robot resources and the determination of their various roles. To fulfill this responsibility, the commander requires all available information about the fire scene in order to make correct tactical decisions about the team's operations. This requires reliable communications at all times with firefighters and robots deployed on the scene.

UAVs can collect information from the air about the fire that is impossible for humans or ground-based robots to obtain. In addition, because they operate in the air above many physical obstacles, they can serve to relay communications between firefighters, robots, and the field commander, all of whom may be separated by long distance in remote locations without physical cellular communication infrastructure.

Mobile network operators (MNO) can be important resources for communications in disaster events such as fires, and when available will be essential partners in the overall response. When available, MNOs can provide backhaul services between the remote scene and a city command center. However, cellular coverage in remote forested areas is often weak or non-existent, and even when present the MNO may only be able to provide voice or other low-rate data but not high-data-rate communication involving images and video.

3.3.4.2. Network slice management for forest firefighting

There are a variety of communication needs and priorities in a firefighting operation, and resources must be allocated to the available network slices in accordance with these needs and priorities. Commands from the operations center or field commander to UAVs and robots will require URLLC. Transfer of images and video will require high bandwidth and low latency, but with a delay requirement that is not as stringent as for command messages. Network slicing will be a critical component in any communication system used to support firefighting operations in order to make sure that the needs of all parties are met.

In this use case, we explain how network slicing can be used to allocate the available resources for communication links with differing latency, bandwidth and packet loss requirements. Figure 19 gives an example of the type of network slices that could be created in a firefighting scenario with UAVs, robots, as well as humans on the scene.

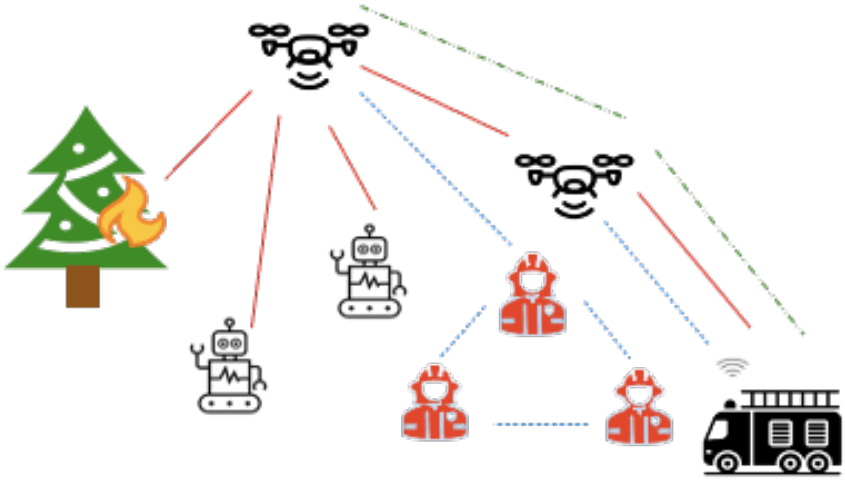

Figure 19: Illustration of drone-assisted for network slicing. Creative Commons: Drone, fire, truck icons based on icons by Felix Westphal, Vector Point, respectively, from thenounproject.com

Firefighters will possess UEs and will be given a very high reliability network slice.

Robots will also have UEs as part of their technology suite, and network slices will be allocated to them with variable latency criteria that depends on their role, whether it be for sensing, communication, or otherwise. Some robots will be equipped with BS-like capabilities (gNBs, or Next Generation Node Bs) and their role will be to allocate the network resources to various personnel as well as robots and UAVs.

UAVs are also equipped with UEs or as gNBs, and their control must be provided by a URLLC link. When MNO support is available, its network slice manager can ensure that the UAV can be linked to the rest of the system via such a URLLC link.

The field commander will be in a location that has an available gNB as well as multi-access edge computing resources and will be able to exert control of the network slices. Constant connectivity to the control center is critical should there be rapid changes to the situation at the fire site, so a fully capable wireless backhaul link must be available for his/her use.

URLLC communications are essential for managing the operation of the UAVs and robots, and this requires that their communication links be allocated dedicated network slices. On the other hand, voice communications use less bandwidth and have a high tolerance for packet loss, which has important implications for the resources that are assigned to them. The different levels of communication need for the various system components makes network slicing a must in order to achieve an efficient use of the network resources.

The specifications relevant to this application can be divided into three levels: operational, functional, and technical requirements. Each of these layers is described below.

3.3.4.2.1. Operational Requirements

The network supports slicing and transport sharing via the Radio Access Network (RAN), and should have sufficient capacity to meet the bandwidth needs of the various network users.

3.3.4.2.2. Functional Requirements

Software-defined networking (SDN) and network slicing are enabled by network switches between the gNBs and the mobile core network.

3.3.4.2.3. Technical Requirements

Some of these requirements have already been mentioned: uplink control signals to UAVs and downlink sensor data from the UAVs (video, images, etc) necessitate a reliable communication link with the mobile command unit, a wireless backhaul must be provisioned between the mobile command unit and the home command center, etc.

3.3.4.3. NOMA in integrated access and backhaul (IAB)

Mobile wireless traffic is growing exponentially due to the huge increase in the number of wireless devices. Cell sizes are shrinking and as a result the number of base stations is increasing in order to deal with this growth [89]. While such network densification is helpful, it is insufficient to meet the exploding demand, and carries with it the need for an ever increasing amount of optical fiber backhauls [90]. New methods for increasing capacity and spectral efficiency are required for new 5G-and-beyond systems [91]. Wireless backhauling is a possible solution to overcome the costs and infrastructure required for fiber-optical backhaul approaches. To this end, NOMA is being considered for IAB nodes as one method for increasing spectral efficiency.

4. Methodological tools

This section provides an overview of methodological tools that are useful in the scope of WP2. Specifically, section 4.1 provides information on the Massive MIMO testbed 'MATE' at Chalmers University of Technology, Section 4.2 overviews the RF waveform lab also located at Chalmers University of Technology, Section 4.3 details the NI high-bands testbed located at NI Dresden GmbH, and Section 4.4 briefly discusses stochastic geometry as a performance evaluation mathematical tool, and provides information on the labs at Chalmers University of Technology along with software, platforms, and simulation tools available for use there.

4.1. Massive MIMO testbed at Chalmers

The MATE testbed at Chalmers is a 28 GHz massive MIMO-capable transceiver system with 2 GHz real time bandwidth that can be utilized for arbitrary waveform applications such as massive MIMO and radar systems.
https://www.chalmers.se/en/projects/Pages/Massive-MIMO-test-bed.aspx

The MATE testbed has two versions up and running, whereof one use low-gain patch antennas and the other use high-gain slotted waveguide antennas. The testbed is currently based on a lab bench and can be accessed via a web-portal for anyone to experiment with high-end microwave hardware and software.

The MATE testbed has recently been upgraded with generation 2 of the analog RF frontend, with improvements on local oscillator leakage, gain and noise levels. Further, high-gain antennas (>30 dBi) have been designed, for enabling MIMO communication on larger distances. Version 2 has been thoroughly characterized and optimized, and 8 receive and 8 transmit antennas can now be used for MIMO experiments. Over-the-air characterization of the testbed has been performed, w.r.t. transmitter and receiver nonlinearities. In connection to the testbed, a simulator has been developed to accurately model the hardware in the testbed.

4.2. RF waveform lab at Chalmers

The RF WebLab at Chalmers allows for online RF measurements of waveforms over a real amplifier, http://dpdcompetition.com/rfweblab/. This makes it possible for those that do not have access to equipment yet to make waveform measurements using a state-of-art experimental setup and thereby increase the understanding of hardware imperfections on signal quality in modern communication system transmitters and enabling comparisons between various algorithms on a common platform.

Remote access to a state-of-the-art waveform measurement setup was initially intended for the competitors of the IEEE International Microwave Symposium (IMS) Student Competition 2014 and 2015. Based on sponsoring of

dedicated measurement equipment from National Instruments, the RF WebLab at Chalmers has become permanently available for everyone to use.

There are two ways to use the platform. One way is to upload a set of data to the server, wait for a few seconds until a measurement has been done, and then download the resulting output data and efficiency data. The other way is to download a dedicated MATLAB .m file or a LabVIEW VI file that handles the entire process.

4.3. NI testbed in high bands overview

In this section an overview about the planned mmWave transceiver architecture is given. It is part of the experimentation system to demonstrate the 5G NR capabilities for beam-based transmissions and smooth coexistence of 5G NR with other mmWave systems. The mmWave link will be based on the NI 5G NR mmWave node including the radio frequency and antenna part as well as a Layer 1 implementation following the 5G NR standard that allows for high throughput and low latency.

In Section 4.3.1 , the RF part of the possible system architecture is described. Section 4.3.2 provides information about the existing IF and mmWave components including their key performance data which are relevant to meet the required system performance. The plan is to start the experimentation at 28 GHz. Then, extend the work to higher frequencies such as 60 GHz. As a result, the mmWave components of 28 GHz only will be presented in this deliverable. For the higher frequencies, the selection of the proper hardware needs more exploration.

4.3.1. System Architecture

Figure 20 shows the mmWave system architecture [92]. The mmWave components will be integrated with NI USRP devices. Hence, the NI USRP serves as IF transmitter/receiver which is connected to up-/downconverters to shift the IF signal into the RF frequency range. Active antenna arrays are used to radiate the RF signals. The presented architecture extends the Sub-7 GHz SDR platform towards mmWave platform, which enables the mmWave experimentation. The Real-Time Antenna-Array-Agnostic Control (AAC) is capable of interfacing several mmWave antenna arrays to NI USRP. The control path presented in Figure 20 is between an external application and the NI USRP FPGA. External applications can be for example a real-time 5G NR protocol stack consisting of PHY and MAC and further higher-layer functionality.

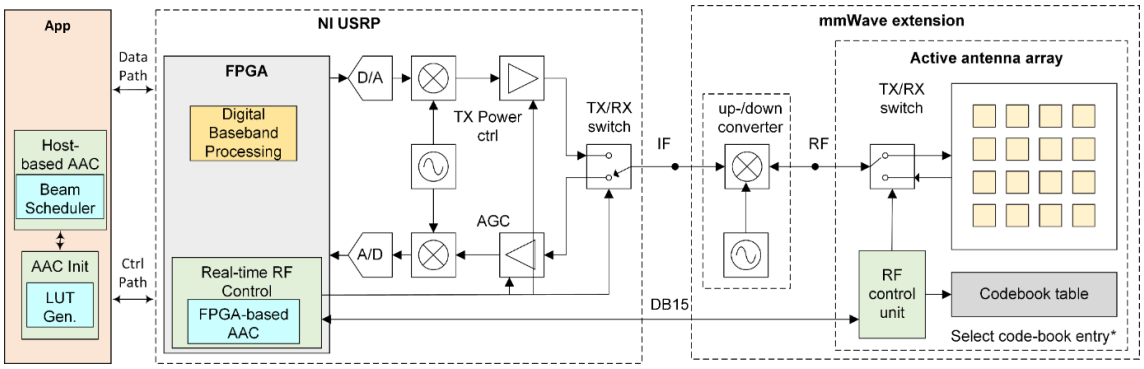

Figure 20: mmWave System Architecture [92]

4.3.2. Description of mmWave System Components

4.3.2.1. PXI System

In the project, a PXI based system is used for mmWave link. The node consists of FPGA processing modules interconnected in a PXI chassis via a high-performance backplane. In addition to the FPGA modules, an RT controller (CPU) is integrated where an NI Linux RT system is running, which is controlling the PXI system and is running PHY related procedures. A C/C++ based higher layer protocol stack can run on the RT controller or on a separate PC. To connect the NI mmWave platform to external devices, a 10 Gbit Ethernet interface is available to feed in and out data on high data rates.

4.3.2.2. NI USRP

The new NI ETTUS USRP X410 provides an integrated hardware and software solution. The hardware architecture combines two daughterboard slots covering 1 MHz – 7.2 GHz with up to 400 MHz of instantaneous real-time bandwidth, multiple high-speed interface options (PCIe Gen 3 x8, dual QSFP28 - 100/10/1 GbE) and double the FPGA resources. It has four channels and supports RFSoC. The USRP X410 supports precise synchronization (10 MHz / PPS). It is equipped with a GPS-disciplined 10 MHz OCXO reference clock. The GPS disciplining provides a high-accuracy frequency reference, and global timing alignment to within 5 ppb when synchronized to the GPS system. The USRP X410 device supports the open source (UHD, RFNoC, GNU Radio, C++, Python) and LabVIEW FPGA, which supports creating custom FPGA implementations and configuring the device using Instrument Design Libraries. Table 1 shows the key performance data of USRP X410. The front panel of USRP X410 is shown in Figure 21.

Figure 21: NI ETTUS USRP X410 Front panel

Parameter	***NI Ettus USRP X410***
Frequency	1 MHz – 7.2 GHz
Bandwidth	400 MHz
Number of Channels	4 Rx, 4 Tx
Max. Power	Tx up to 22 dBm[1] - Rx 0 dBm
DAC resolution	14 bit
ADC resolution	12 bit
Interface Options	Dual QSFP28 (100/10/1 GbE), PCIe Gen 3 x8[2]
Onboard IP	SD-FEC, DDC, DUC
Synchronization	Onboard GPS DO
SW Support	GNURadio, LabVIEW[2], RFNoC, C++, Python,
Key Features	RFSOC Based, 5G Ready, Wide Band, Multi-Channel

Table 1: NI ETTUS USRP X410 key performance data.

4.3.2.3. Up-/Down- Converters

For the 28 GHz exploration, the RF 5G Mixer is a 24 GHz to 28 GHz up / down converter with an integrated phase locked loop synthesizer. It contains a MMIC mixer, a synthesizer with integrated VCO, a differential 100 MHz reference TCXO, and a loop filter. The up- and downconverter is going to be used on the gNB side in combination with the 8x8 active antenna array. The IF carrier frequency can be up to 4 GHz. Table 2 shows the specifications of up / down converter. Figure 22 shows the up and down converter.

Upconverter		***Downconverter***	
IF	DC … 4 GHz	IF	DC … 4 GHz
RF	24 … 28 GHz	RF	24 … 28 GHz

[1] See specification for details.
[2] Available in September 2021.

Conversion loss	Typically 14 dB	Conversion loss	Typically 15 dB
IF input 1dB compression point	6 dBm	RF input 1dB compression point	14 dBm
Isolation IF to RF	Typically 41 dB	Isolation RF to IF	Typically 29 dB

Table 2: Key performance data for up- and down converter to/from 28 GHz.

Figure 22: The 28G Up- and Down- converter

4.3.2.4. Active antenna arrays for gNB and UE

The mmWave antenna arrays are designed for the 28G band. They cover a frequency range of 26.5 to 28.5 GHz and have a linear polarization. Only the TDD operation mode is supported. The beam widths are fixed. On the gNB side, an 8x8 active antenna array will be used while on the UE side, a 2x8 active antenna array will be used. The antenna array of gNB does not include the LO and the up / down converter; their hardware is separated as it is described above. The 2x8 active antenna array of UE is occupied with an integrated up/down converter, an LO and a microcontroller (MCU) to achieve beamforming functionality. Both provide a 2D electronic beam scan. The control of the active antenna arrays will be done via the USRP using UART and SPI protocols for the 8x8 active antenna array and using UART for the 2x8 active antenna array. Table 3 shows the specifications of the gNB and UE antenna arrays. The front panel of the 8x8 active antenna array is shown in Figure 23.

8x8 active antenna array (for gNB)		**2x8 active antenna array (for UE)**	
RF	26.5 … 28.5 GHz	RF	26.5 … 28.5 GHz

Input 1 dB compression point	0 dBm	Input 1 dB compression point	+3 dBm
TX/RX gain	50 dB	TX/RX gain	40 dB
Polarization	Vertical linear	Polarization	Vertical linear
Beam coverage	+/- 60° AZ/EL each	Beam coverage	+/-60° AZ, +/-15° EL
Default beam width	15°	Beam width	15°
Number of simultanous beams	Single radiation beam	Number of simultanous beams	Single radiation beam
Beam update rate	3 us	Beam update rate	100 us
RF Interface	TDD only	RF Interface	TDD only
Control Interfaces	UART, SPI	Control Interfaces	UART

Table 3: Key performance data for 8x8 and 2x8 active antenna arrays.

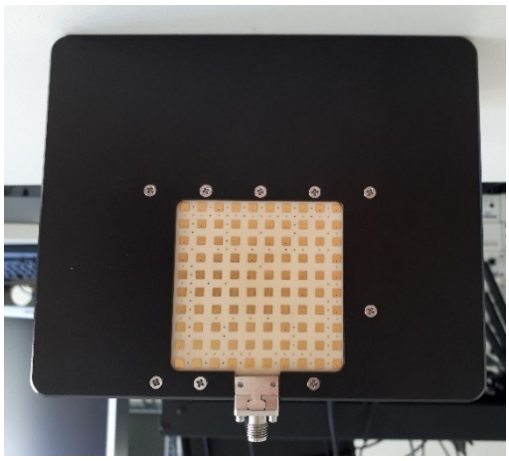

Figure 23: The 8x8 Active antenna array.

4.4. Other tools

In this section mathematical tools used for performance evaluation will be discussed. More specifically, section 4.4.1 will provide a brief overview of stochastic geometry, while section 4.4.2 provides information on the equipment of the Chalmers University of Technology labs, that are available to the consortium.

4.4.1. Stochastic Geometry

SG is a mathematical tool that can be used for wireless network modelling, analysis, and optimization particularly useful for system level analysis [93] even for Heterogeneous deployments. SG allows us to derive closed form expression for a metric of interest, while considering specific known parameters of the system [94]. Usually, in the context of this deliverable, the focus would be on a performance metric, like the coverage probability, the system capacity etc. allowing for exploration of various evaluation and analysis targets, like rate analysis, interference management analysis, system coverage analysis, rate/capacity analysis, mmWave link performance evaluation etc.

With SG we can model a wireless communication system assuming a geographical area (a 2-D plane) on which we distribute randomly *points.* These points have specific known characteristics, and we define a collection of such points a *point process*. A point process follows a distribution, and the most popular point process used for wireless communication systems modelling is a *Poisson* point process (PPP) as seen from the selected publications in section 3.2.2. The points used in such a case are instances of a random variable that follows a Poisson distribution and can model BSs, UEs etc. according to a density value λ, defined in device number/ area measure.

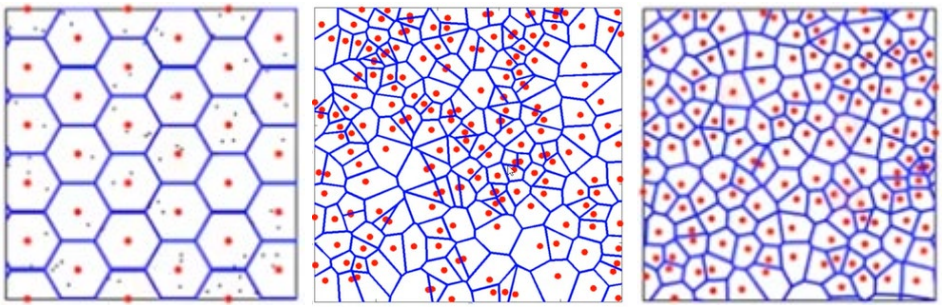

Figure 24: From left to right: Traditional grid, PPP distribution, Real 4G deployment [93]

So far, in textbooks, the main approach in representing a wireless communication system was that of a hexagonal grid with evenly distributed BSs in the area, which is an oversimplification and is not very realistic as seen in Figure 24. In contrast, the SG modelling under a PPP distribution is closer to the real-life deployments as seen also in Figure 24. The problem with the traditional grid model as discussed in [93] is that the hexagonal grid model deviates from reality. Additionally, due to the hexagonal assumption of a cell the maths are difficult to solve and there is no scalability. In contrast, when using SG, usually the BSs locations are modelled according to a PPP and the maths are easier to solve towards a closed form expression. That is one of the main reasons SG has been widely used in the past years for performance evaluation and analysis of communication systems. One problem that might arise with SG is that the interference of nearly spaced BSs might be overestimated (as due to the exponential nature of the Poisson distribution, points might be closely spaced) as

seen in Figure 24. In general, SG with the aid of relevant theorems, allows for computing closed-forms of the Laplace transformation and the probability density function (pdf) of the metric that was chosen to analyse making it an important tool that allows for rigorous analysis of wireless communication systems.

4.4.2. Chalmers Labs

Chalmers has modern laboratories with numerous workstations, C3SE simulation cluster (www.c3se.chalmers.se), and various simulation software (MATLAB, OPNET, NS-3, IT++, etc.).

IT++ (http://itpp.sourceforge.net/4.3.1/) is a C++ library of mathematical, signal processing and communication classes and functions, originating from Chalmers University of Technology, Gothenburg, Sweden, and released under the terms of the GNU General Public License (GPL). Its main use is in simulation of communication systems and for performing research in the area of communications.

IT++ is being developed and widely used by researchers who work in the area of communications, both in the industry and at universities. In 2005, 2006 and 2007, it was further developed as a part of the European Network of Excellence in Wireless Communications (NEWCOM). The kernel of the library consists of generic vector and matrix classes, and a set of accompanying routines. Such a kernel makes IT++ similar to MATLAB, GNU Octave or SciPy. IT++ makes an extensive use of existing open-source or commercial libraries for increased functionality, speed and accuracy. It is possible to compile and use IT++ without any of the above listed libraries, but the functionality will be reduced. IT++ should work on GNU/Linux, Sun Solaris, Microsoft Windows (with Cygwin, MinGW/MSYS or Microsoft Visual C++) and Mac OS X operating systems.

5. References

[1] F. Boccardi, R. W. Heath, A. Lozano, T. Marzetta and P. Popovski, “Five disruptive technology directions for 5G,” *IEEE Communications Magazine,* vol. 52, no. 2, pp. 74-80, Feb. 2014.

[2] G. Liu, Y. Huang, Z. Chen, L. Liu, Q. Wang and N. Li, “5G Deployment: Standalone vs. Non-Standalone from the Operator Perspective,” *IEEE Communications Magazine,* vol. 58, no. 11, pp. 83-89, Nov. 2020.

[3] 3GPP, 2021. [Online]. Available: https://www.3gpp.org.

[4] M. Shafi, A. Molisch, P. J. Smith, T. Haustein, P. Zhu, P. De Silva, F. Tufvesson, A. Benjebbour and G. Wunder, “5G Tutorial Overview of Standards, Trials, Challenges, Deployement, and Practice,” *IEEE Journal on Selected Areas in Communications,* vol. 35, no. 6, pp. 1201-1221, Jun. 2017.

[5] J. Peisa, P. Persson, S. Parkvall, E. Dalhman, A. Grøvlen, C. Hoymann and D. Gerstenberger, “5G evolution: 3GPP Releases 16&17 Overview,” Ericsson Technology Review, 2020.

[6] S. Parkvall, E. Dahlmann, A. Furuskar and M. Frenne, “NR: The New 5G Radio Access Technology,” *IEEE Communications Standards Magazine,* vol. 1, no. 4, pp. 24-30, Dec. 2017.

[7] X. Wang, L. Kong, F. Kong, F. Qiu, M. Xia, S. Arnon and G. Chen, “Millimeter wave Communication: A Comprehensive Survey,” *IEEE Communications Surveys & Tutorials,* vol. 20, no. 3, pp. 1616-1653, 2018.

[8] Z. Pi and F. Khan, “An Introduction to MIllimeter-Wave Mobile Broadband Systems,” *IEEE Communications Magazine,* vol. 49, no. 6, pp. 101-107, 2011.

[9] M. Williamson, G. Athanasiadou and A. Nix, “Investigating The Effects of Antenna Directivity on Wireless Indoor Communication at 60 Ghz,” *Proceedings of 8th International Symposium on Personal, Indoor and Mobile Radio Communications,* vol. 97, no. 2, pp. 635-639, 1997.

[10] X. Zhou, Z. Zhang, Y. Zhu, Y. Li, S. Kumar, A. Vahdat, B. Zhao and H. Zheng, “Mirror Mirror on the Ceiling: Flexible Wireless Links for Data Centers,” *ACM SIGCOMM Computer Communication Review,* vol. 42, no. 4, pp. 443-454, 2012.

[11] W. Zhang, X. Zhou, L. Yang, Z. Zhang, B. Zhao and H. Zheng, “3D Beamforming for Wireless Data Centers,” *Proceedings of the 10th ACM workshop on hot topics in networks,* Nov. 2011.

[12] T. S. Rappaport, R. W. Heath, R. C. Daniels and J. N. Murdock, Millimeter wave wireless communications, Prentice Hall, 2015.

[13] T. S. Rappaport, S. Sun, R. Mayzus, H. Zhao, Y. Azar, K. Wang, G. N. Wong, J. K. Schulz, M. Samimi and F. Gutierrez, “Millimeter Wave Mobile

Communications for 5G Cellular: It Will Work!," *IEEE Access,* vol. 1, pp. 335-349, 2013.

[14] T. L. Marzetta, "Noncooperative Cellular Wireless with Unlimited Number of Base Station Antennas," *IEEE Transactions on Wireless COmmunications,* vol. 9, no. 11, pp. 3590-3600, Nov. 2010.

[15] T. L. Marzetta, E. Larsson, H. Yang and H. Ngo, Fundamentals of Massive MIMO, Cambridge University Press, 2016.

[16] E. Björnson, J. Hoydis and L. Sanguinetti, "Massive MIMO Networks: Spectral, Energy and Hardware Efficiency," *Foundations and Trends in Signal Processing,* vol. 11, no. 3-4, pp. 154-655, 2017.

[17] Samsung, "Massive MIMO for New Radio," Dec. 2020. [Online]. Available: https://tinyurl.com/erfznu2x. [Accessed 14 05 2020].

[18] X. You, D. Wang and J. Wang, Distributed MIMO and Cell-Free Mobile Communication, Springer, 2021.

[19] Ö. T. Demir, E. Björnson and L. Sanguinetti, "Foundations of User-Centric Cell-Free Massive MIMO," *Foundations and Trends® in Signal Proccesing,* vol. 14, no. 3-4, pp. 162-472, 2021.

[20] Ericsson, "Radio Stripes: re-thinking mobile networks," Feb. 2019. [Online]. Available: https://www.ericsson.com/en/blog/2019/2/radio-stripes. [Accessed 14 05 2019].

[21] 3GPP, "TS 38.211(v16.05.0): Physical channels and modulation," 2021.

[22] Keysight Technologies, "Top 5 Challenges for 5G New Radio," Oct. 2018. [Online]. Available: https://www.keysight.com/zz/en/assets/7018-06373/white-papers/5992-3417.pdf. [Accessed 14 05 2021].

[23] Ericsson Technology Review, "5G New Radio: Designing for the Future," 2017. [Online]. Available: https://www.ericsson.com/en/reports-and-papers/ericsson-technology-review/articles/designing-for-the-future-the-5g-nr-physical-layer. [Accessed 14 05 2021].

[24] 3GPP, "TR 38.802 (v14.2.0): Study on New Radio Access Technology, Physical Layer Aspects," 2017.

[25] 3GPP, "TR 38.912 (v16.0.0): Study on New Radio (NR) access technology," 2020.

[26] 3GPP, "R1-1609663:On the mini-slot structure," 2016.

[27] N. Bhushan, T. Ji, O. Koymen, J. Smee, J. Soriaga, S. Subramanian and Y. Wei, "Industry Perspective: 5G Air Interface System Design Principles," *IEEE Wireless Communications,* vol. 24, no. 5, pp. 6-8, Oct. 2017.

[28] H. Sadia, M. Zeeshan and S. A. Sheikh, "Performance Analysis of Downlink Power Domain NOMA under Fading Channels," *2018 ELEKTRO,* 2018.

[29] T. M. Cover and A. Joy, Elements of Information Theory, College of New York, 1991.

[30] D. Duchemin, J. Gorce and C. Goursaud, “Code Domain non Orthogonal Multiple Access versus ALOHA: A Simulation-based Study,” *25th Inthernational Conference on Telecommunications (ICT),* 2018.

[31] Islam, S., M. Zeng, and O.A. Dobre, “NOMA in 5G systems: Exciting possibilities for enhancing spectral efficiency,” *IEEE 5G Tech Focus,* vol. 1, no. 2, June 2017.

[32] Ding, Z. and H.V. Poor, “Design of massive-MIMO-NOMA with limited feedback,” *IEEE Signal Processing Letters,* vol. 23, no. 5, pp. 629-633, 2016.

[33] Liu, X., et al , “Spectrum resource optimization for NOMA-based cognitive radio in 5G communications,” *IEEE Access,* vol. 6, pp. 24904-24911, 2018.

[34] Chen, J., L. Yang, and M.-S. Alouini, “ Physical layer security for cooperative NOMA systems,” *IEEE Transactions on Vehicular Technology,* vol. 67, no. 5, pp. 4645-4649, 2018.

[35] S. Coleri, M. Ergen, A. Puri and A. Bahai, “Channel estimation techniques based on pilot arrangement in OFDM systems,” *IEEE Transactions on Broadcasting,* vol. 48, no. 3, pp. 223-229, Sept. 2002.

[36] W. Sheen and G. L. Stuber, “MLSE equalization and decoding for multipath-fading channels,” *IEEE Transactions on Communications,* vol. 39, no. 10, pp. 1455-1464, Oct. 1991.

[37] J. van de Beek, O. Edfors, M. Sandell, S. K. Wilson and P. O. Borjesson, “On channel estimation in OFDM systems,” *1995 IEEE 45th Vehicular Technology Conference Countdown to the Wireless Twenty-First Century,* vol. 2, pp. 815-819, 1995.

[38] O. Elijah, C. Y. Leow, T. A. Raahman, S. Nunoo and S. Z. Iliya, “A Comprehensive Survey of Pilot COntamination in Massive MIMO 5G System,” *IEEE Communications Surveys & Tutorials,* vol. 18, no. 2, pp. 905-923, 2016.

[39] X. Rao and V. K. N. Lau, “Distributed COmpressive CSIT Estimation and Feedback for FDD Multi-User Massive MIMO Systems,” *IEEE Transactions on Signal Processing,* vol. 62, no. 12, pp. 3261-3271, June 2014.

[40] J. Choi, D. J. Love and P. Bidigare, “Downlink Training Techniques for FDD Massive MIMO Systems: Open-Loop and CLosed-Loop Training With Memory,” *IEEE Journal of Selected Topics in Signal Processing,* vol. 8, no. 5, Oct. 2014.

[41] R. W. Heath, N. González-Prelcic, S. Rangan, W. Roh and A. M. Sayeed, “An Overview of Signal Processing Techniques for MIllimeter Wave

MIMO Systems," *IEEE Journal of Selected Topics in Signal Processing,* vol. 10, no. 3, pp. 436-453, April 2016.

[42] J. Mo and R. W. Heath, "Capacity Analysis of One-Bit Quantized MIMO Systems with Transmitter Channel State Information," *IEEE Transactions on Signal Processing,* vol. 63, no. 20, pp. 5498-5512, Oct. 2015.

[43] L. Dai, X. Gao, S. Han, I. Chih-Lin and X. Wang, "Beamspace channel estimation for milimeter-wave massive MIMO systems with lens antenna array," *2016 IEEE/CIC International COnference on Communication in China (ICCC),* pp. 1-6, 2016.

[44] I. Goodfellow, Y. Bengio, A. Courville and Bengio Y., Deep learning, Cambridge: MIT Press, 2016.

[45] Z. Qin, H. Ye, G. Y. Li and B. F. Juang, "Deep Learning in Physical Layer Communications," *IEEE Wireless Communications,* vol. 26, no. 2, pp. 93-99, April 2019.

[46] H. Ye, G. Y. Li and B. Juang, "Power of Deep Learning for Channel Estimation and Signal Detection in OFDM Systems," *IEEE Wireless Communications Letters,* vol. 7, no. 1, pp. 114-117, Feb. 2018.

[47] P. Dong, H. Zhang, G. Y. Li, I. S. Gaspar and N. Naderi-Alizadeh, "Deep CNN-Based Channel Estimation for mmWave Massive MIMO Systems," *IEEE Journal of Selected Topics in Signal Processing,* vol. 13, no. 5, pp. 989-1000, Sept. 2019.

[48] E. Balevi, A. Doshi and J. G. Andrews, "Massive MIMO Channel Estimation with an Untrained Deep Neural Network," *IEEE Transactions on Wireless Communications,* vol. 19, no. 3, pp. 2079-2090, Mar. 2020.

[49] D. Ulyanov, A. Vedaldi and V. Lempitsky, "Deep Image Prior," *Proceedings of the IEEE COnference on COmputer VIsion and Pettern Recognition (CVPR),* pp. 9446-9454, 2018.

[50] M. Soltani, V. Pourahmadi, A. Mirzaei and H. Sheikhzadeh, "Deep Learning-based Channel Estimation," *IEEE Communications Letters,* vol. 23, no. 4, pp. 652-655, Apr. 2019.

[51] Y. Zhang, M. Alrabeiah and A. Alkhateeb, "Deep Learning for Massive MIMO with 1-bit ADCs: When More Antennas Need Fewer Pilots," *IEEE Wireless Communications Letters,* vol. 9, no. 8, pp. 1273-1277, Aug. 2020.

[52] Y. Jin, J. Zhang, B. Ai and X. Zhang, "Channel Estimation for mmWave Massive MIMO with ConvolutionalBlind Denoising Network," *IEEE Communications Letters,* vol. 24, no. 1, pp. 95-98, Jan. 2020.

[53] M. Albrabeiah and A. Alkhateeb, "Deep Learning for TDD and FDD Massive MIMO: Mapping Channels in Space and Frequency," *2019 53rd Asilomar Conference on SIgnals, Systems and Computers,* pp. 1465-1470, 2019.

[54] Y. Yang, F. Gao, G. Y. Li and M. Jian, “Deep Learning-Based Downlink Channel Prediction for FDD Massive MIMO System,” *IEEE COmmunication Letters,* vol. 23, no. 11, pp. 1994-1998, Nov. 2019.

[55] C. Wen, W. Shih and S. Jin, “Deep Learning for Massive MIMO CSI Feedback,” *IEEE Wireless Communications Letters,* vol. 7, no. 5, pp. 748-751, Oct. 2018.

[56] C. Chun, J. Kang and I. Kim, “Deep Learning-Based Channel Estimation for Massive MIMO Systems,” *IEEE Wireless Communications Letters,* vol. 7, no. 5, pp. 1228-1231, Aug. 2019.

[57] C. Huang, G. C. Alexandropoulos, A. Zappone, C. Yuen and M. Debbah, “Deep Learning for UL/DL Channel Calibration in Generic Massive MIMO Systems,” *2019 IEEE International COnference on COmmunications (ICC),* pp. 1-6, 2019.

[58] E. Basar, M. Di Renzo, J. De Rosny, M. Debbah, M. -S. Alouini and R. Zhang, “Wireless Communications Through Reconfigurable Intelligent Surfaces,” *IEEE Access,* vol. 7, pp. 116752-116773, 2019.

[59] C. Holloway, E. F. Kuester, J. A. Gordon, J. O'Hara, J. Booth and D. R. Smith, “An overview of the Theory and Applications of Metasurfaces: The Two-Dimensional Equivalents of Metamaterials,” *IEEE Antennas and Propagation Magazine,* vol. 54, no. 2, pp. 10-35, Apr. 2012.

[60] Z. Wang, L. Liu and S. Cui, “Channel Estimation for Intelligent Reflecting Surface Assisted Multiuser Communications: Framework, Algorithms, and Analysis,” *IEEE Transactions on Wireless Communications,* vol. 19, no. 10, pp. 6607-6620, Oct. 2020.

[61] Z. He and X. Yuan, “Cascaded Channel Estimation for Large Intelligent Metasurface Assisted Massive MIMO,” *IEEE Wireless Communications Letters,* vol. 9, no. 2, pp. 210-214, Feb. 2020.

[62] Y. Yang, B. Zheng, S. Zhang and R. Zhang, “Intelligent Reflecting Surface Meets OFDM: Protocol Design and Rate Maximization,” *IEEE Transactions on Communications,* vol. 68, no. 7, pp. 4522-4535, Jul. 2020.

[63] J. Chen, Y. C. Liang, H. V. Cheng and W. Yu, “Channel Estimation for Reconfigurable Intelligent Surface Aided Multi-User MIMO Systems”.*arXiv:1912.03619.2019.*

[64] A. Taha, M. Alrabeiah and A. Alkhateeb, “Enabling Large Intelligent Surfaces with Compressive Sensing and Deep Learning,” *IEEE Access,* vol. 9, pp. 44304-44321, 2021.

[65] Ö. Özdogan and E. Björnson , “Deep Learning-based Phase Reconfiguration for Intelligent Reflecting Surfaces,” *arXiv:2009.13988,* Sept. 2020.

[66] J. Gao, C. Zhong, X. Chen, H. Lin and Z. Zhang, “Unsupervised Learning for Passive Beamforming,” *IEEE Communications Letters,* vol. 24, no. 5, pp. 1052-1056, May 2020.

[67] T. L. Jensen and E. de Carvalho, “An Optimal Channel Estimation Scheme for Intelligent Reflecting Surfaces Based on a Minimum Variance Unbiased Estimator,” *2020 IEEE International Conference on Acoustics, Speech and Signal Processing (ICASSP),* pp. 5000-5004, 2020.

[68] A. M. Elbir, A. Papazafeiropoulos, P. Kourtessis and S. Chatzinotas, “Deep Channel Learning for Large Intelligent Surfaces Aided mm-Wave Massive MIMO Systems,” *IEEE Wireless Communications Letter,* vol. 9, no. 9, pp. 1447-1451, Sept. 2020.

[69] S. Shamai and B. Zaidel, “Enhancing the cellular downlink capacity via coprocessing at the transmitting end,” *IEEE VTS 53rd Vehicular Technology Conference,* vol. 3, pp. 1745-1749, Spring 2001.

[70] X. You, D. Wang, B. Sheng, X. Gao, X. Zhao and M. Chen, “Cooperative distributed antenna systems for mobile communications [Coordinated and Distributed MIMO],” *IEEE Wireless Communications,* no. 3, pp. 35-43, Jun. 2010.

[71] E. Björnson and L. Sanguinetti, “A New Look at Cell-Free Massive MIMO: Making it Practical with Dynamic Cooperation,” *IEEE 30th Annual International Symposium on Personal, Indoor and Mobile Radio Communications (PIMRC),* pp. 1-6, 2019.

[72] H. Q. Ngo, A. Ashikhmin, H. Yang, E. G. Larsson and T. L. Marzetta, “Cell-free Massive MIMO versus small cells,” *IEEE Transactions on Wireless Communications,* vol. 16, no. 3, pp. 1834-1850, 2017.

[73] S. Buzzi and C. D'Andrea, “Cell-free massive MIMO: User-centric Approach,” *IEEE Communication Letters,* vol. 6, no. 6, pp. 706-709, 2017.

[74] G. Interdonato, E. Bjornson, H. Q. Ngo, P. Frenger and E. G. Larsson, “Ubiquitous cell-free massive MIMO communications,” *EURASIP J Wireless Com Network,* vol. 2019:197, Dec. 2019.

[75] A. Papazafeiropoulos, P. Kourtessis, M. D. Renzo, S. Chatzinotas and J. M. Senior, “Performance Analysis of Cell-Free Massive MIMO Systems: A Stochastic Geometry Approach,” *IEEE Transactions on Vehicular Technology,* vol. 69, no. 4, pp. 3523-3537, April 2020.

[76] J. Shi, C. Pan, W. Zhang and M. Chen, “Performance Analysis for User-Centric Dense Networks With mmWave,” *IEEE Access,* pp. 14537-14548, 2019.

[77] K. Hosseini, W. Yu and R. S. Adve, “A Stochastic Analysis of Network MIMO Systems,” *IEEE Transactions on Signal Processing,* vol. 64, no. 16, Aug. 2016.

[78] S. R. Islam, N. Avazov, O. A. Dobre and K. S. Kwak, “Power-domain Non-Orthogonal Multiple Access (NOMA) in 5G Systems: Potentials and Challenges,” *IEEE Communications Surveys & Tutorials,* vol. 19, no. 2, pp. 721-742, 2016.

[79] Timotheou, S. Timotheou and I. Krikidis, “Fairness for Non-Orthogonal Multiple Access in 5G Systems,” *IEEE Signal Processing Letters,* vol. 22, no. 10, pp. 1647-1651, 2015.

[80] Z. Yang, Z. Ding, P. Fan and G. K. Karagiannidis, “On the Performance of Non-Orthogonal Multiple Access Systems with Partial Channel Information,” *IEEE Transactions on Communications,* vol. 64, no. 2, pp. 654-667, 2015.

[81] Z. Ding, F. Adachi and H. V. Poor, “The Application of MIMO to Non-Orthogonal Multiple Access,” *IEEE Transactions on Wireless Communications,* vol. 15, no. 1, pp. 537-552, 2016.

[82] F. Tonini, C. Natalino, M. Furdek, C. Raffaelli and P. Monti, “Network Slicing Automation: Challenges and Benefits,” *2020 International Conference on Optical Network Design and Modeling (ONDM),* 2020.

[83] P. Rost, C. Mannweiler, D. S. Michalopoulos, C. Sartori, V. Sciancalepore, N. Sastry, O. Holland, S. Tayade, B. Han, D. Bega, D. Aziz and H. Bakker, “Network Slicing to Enable Scalability and Flexibility in 5G Mobile Networks,” *IEEE Communications Magazine,* vol. 55, no. 5, pp. 72-79, 2017.

[84] S. W. Running, “Is Global Warming Causing More, Larger Wildfires?,” *Science,* vol. 313, pp. 927-928, 2006.

[85] R. Boffard, “Burning Issue [Firefighting Technology],” *Engineering & Technology,* vol. 10, no. 7-8, pp. 48-51, 2015.

[86] D. Lund, D. Corujo and R. Aguiar, “When will 5G be Ready for Use by PPDR,” 2018.

[87] C. C. Grant, A. Jones, A. Hamins and N. Bryner, “Realizing The Vision of Smart Fire Fighting,” *IEEE Potentials,* vol. 34, no. 1.

[88] K. W. Sung, E. Mutafungwa, R. Jäntti, M. Choi, J. Jeon, D. Kim, J. Kim, J. Costa-Requena, A. Nordlöw, S. Sharma, G. Destino, Y. Deng, T. Mahmoodi, M. Ullmann, A. Nachler, Y. Kyung, S. Kim, S. Seo and S. -L. Kim, “PriMO-5G: Making Firefighting Smarter with Immersive Videos Through 5G,” *2019 IEEE 2nd 5G World Forum (5GWF),* 2019.

[89] Y. Zhang, M. A. Kishk and M. -S. Alouini, “A Survey on Integrated Access and Backhaul Networks,” *arXiv: 2101.01286,* 2021.

[90] C. Madapatha, B. Makki, C. Fang, O. Teyeb, E. Dahlman, M. -S. Alouini and T. Svensson, “Integrated Access and Backhaul Networks: Current Status and Potentials,” *IEEE Open Journal of the Communications Society,* vol. 1, pp. 1374-1389, 2020.

[91] H. A. Willebrand and B. S. Ghuman, “Fiber Optics without Fiber,” *IEEE Spectrum,* vol. 38, no. 8, pp. 40-45, 2001.

[92] A. Gaber, A. Nahler, W. Nitzold and M. Anderseck, “USRP-based mmWave Prototyping Architecture with Real-Time RF Control,” *IEEE International Microwave Symposium,* 2021.

[93] D. Xenakis, “Analysis of Multi-tier Wireless Networks using Stochastic Geometry,” *2nd SEMANTIC ITN School on E2E validation of 5G Networks: Key Analytical, Prediction, Simulation, Experimental Tools,* 2021.

[94] A. Tsiota, D. Xenakis, N. Passas, and L. Merakos, On Jamming and Black Hole Attacks in Heterogeneous Wireless Networks, IEEE Transactions on Vehicular Technology, vol. 68, no. 11, pp. 10761-10774, Nov. 2019